Integrative taxonomy clarifies species limits in the hitherto monotypic passion-vine butterfly genera *Agraulis* and *Dryas* (Lepidoptera, Nymphalidae, Heliconiinae)

R A Y N E R   N Ú Ñ E Z[1], K E I T H   R .   W I L L M O T T[2], Y O S I E L   Á L V A R E Z[3],
J U L I O   A .   G E N A R O[4], A N T O N I O   R .   P É R E Z - A S S O[5],
M A R I N A   Q U E J E R E T A[6], T H O M A S   T U R N E R[7],
J A C Q U E L I N E   Y .   M I L L E R[2], C H R I S T I A N   B R É V I G N O N[8],
G E R A R D O   L A M A S[9] and A X E L   H A U S M A N N[1]

[1]SNSB–Zoologische Staatssammlung München, Section Lepidoptera, Munich, Germany, [2]Florida Museum of Natural History University of Florida, Gainesville, FL, U.S.A., [3]Facultad de Biología, Universidad de La Habana, La Habana, Cuba, [4]Florida State Collection of Arthropods, Gainesville, FL, U.S.A., [5]National Museum of Natural History, Santo Domingo, Dominican Republic, [6]Institut de Recherche sur la Biologie de l'Insecte (IRBI), UMR 7261 CNRS/Université de Tours, Tours, France, [7]Caribbean Wildlife Publications, Safety Harbor, FL, U.S.A., [8]Villa A7, Matoury, French Guiana, 97351, France and [9]Museo de Historia Natural, Universidad Nacional Mayor de San Marcos, Lima, Peru

Abstract. The Heliconiini genera *Agraulis* and *Dryas* are widely distributed throughout the Neotropics and into adjacent temperate regions, and although they are currently treated as monotypic, both show significant geographic phenotypic variation. In this work, we employ six genetic markers (4199 bp), two mitochondrial and four nuclear, to perform coalescent species delimitation analyses in Bayesian Phylogenetics and Phylogeography (BPP) and in integrated BPP (iBPP), the latter also includes linear measurements and wings landmarks. We also analyze cytochrome c oxidase I (COI) barcode sequences for each genus using genetic distances, haplotype networks and a character-based approach. Based on the model testing results, complemented with data from previous studies, we performed morphometric analyses to compare fore and hindwing size, aspect ratio and shape among the new species. In addition, we compared the forewing spot pattern of hypothesizes species using the R package *patternize* and, for *Dryas*, compared the colour patterns of mature larvae. Model testing of the molecular species delimitation outputs favoured a seven species hypothesis for *Agraulis* and a four species hypothesis for *Dryas*. Average distances among COI barcode sequences of these groups were from 1.09 to 5.81% in *Agraulis* and from 1.09 to 3.44% in *Dryas*. Within-group distances ranged from 0 to 1.11% and between 0 and 2.43%, respectively. NeighborNet haplotype networks showed that all but one of the species are monophyletic, and the character-based approach found exclusive diagnostic positions for most species, while the rest can be recognized by unique combinations of the 44 informative nucleotide positions analysed. Morphometric analysis supported all species of *Agraulis* and *Dryas* based on wing shape, and also in several cases on wing sizes and aspect ratio (hindwing length–forewing length), including *A. v. galapagensis*, which was absent from the molecular study. The analysis of the forewing spot pattern also revealed differences among most species hypothesis. The colour

[Correction added on 29 October 2021, after first online publication: *D. dominicana* corrected to *D. lucia*.]

pattern of the last instar larva is also diagnostic for each *Dryas* species hypothesis. Locality data for species in both genera show that most of them are allopatric albeit a few have contact zones being parapatric at some locations. Based on the observed genetic differences, which covary with morphology and geographical distribution, we recommend the recognition of eight species of *Agraulis*: *A. incarnata*, *A. vanillae*, *A. forbesi* **new status**, *A. insularis* **reinstated status**, *A. maculosa* **new status**, *A. lucina* **reinstated status**, *A. galapagensis* **new status** and one undescribed species, and four species of *Dryas*: *D. iulia*, *D. dominicana* **revised status**, *D. lucia* **revised status** and *D. alcionea* **reinstated status**. Further work is needed to investigate, which selective forces have led to the current configurations of venation and wing shape, the probable gene flow among species with a focus on *Agraulis* and gather more data on species ecology.

LSIDurn: lsid: zoobank.org: pub: 9E8C9F6E-91C3-4FB2-804D-1A9C4BD2EABB.

Introduction

Passion-vine butterflies of the subfamily Heliconiinae (Lepidoptera: Nymphalidae) have attracted the attention of researchers for a long time. Besides their visual charisma, there are many other reasons for this interest, including their coevolution with passion vines (Passifloraceae), behavioural ecology and mimicry, among other aspects of their biology (Benson *et al.*, 1976; Brown, 1981; Mallet & Gilbert, 1995; Penz & Krenn, 2000). The Heliconiinae have also been the target group of numerous molecular studies during the last few decades, including Brower & Egan (1997), Beltrán *et al.* (2002, 2007), Bull *et al.* (2006), Martin *et al.* (2013), Nadeau *et al.* (2013) and Kozak *et al.* (2015), among many others. However, the vast majority of these works have focused on the subfamily's most species-rich genus, *Heliconius* Kluk.

The genera *Agraulis* Boisduval & Le Conte and *Dryas* Hübner have been largely recognized as monotypic, with both being widespread across the Neotropics (Smith *et al.*, 1994; Lamas, 2004; Rosser *et al.*, 2012; Warren *et al.*, 2017). The morphological variability exhibited by both genera across their distribution is reflected in the current taxonomy, with eight named subspecies recognized for *Agraulis vanillae* and 14 for *Dryas iulia* (Lamas, 2004; Warren *et al.*, 2017). The taxonomy has been based to date only on the adult phenotype (Riley, 1926; Michener, 1942; Emsley, 1963; Clench, 1975; Miller & Steinhauser, 1992) and biogeography, but the immature stages, although described for several subspecies, have not been used in taxonomy (Beebe *et al.*, 1960; Rickard, 1968; Paim *et al.*, 2004; da Silva *et al.*, 2006; Askew & Stafford, 2008; Daniels, 2009). Only recently, North American *Agraulis incarnata* has been recognized as a distinct species after the analysis of COI barcodes and nuclear genomes (Zhang *et al.*, 2020).

Few representatives of *Agraulis* and *Dryas* have been included in molecular studies on the Heliconiinae and Nymphalidae (Wahlberg *et al.*, 2009; Massardo *et al.*, 2014; Kozak *et al.*, 2015). The only exceptions are two large-scale biogeographical studies: one including *A. vanillae* (Runquist *et al.*, 2012, COII data) and the other focused on two Heliconiinae, one of them *D. iulia* (Davies & Bermingham, 2002,

allozyme and COI–II data). Both studies found deep genetic divergences, the first between North and South American populations of *Agraulis*, the second among *Dryas* populations on the West Indies islands and the continent. However, due to their focus, these studies have not proposed formal changes to the taxonomy and classification of the species under consideration.

In the present work, we use two mitochondrial and four nuclear markers to investigate possible cryptic diversity within *Agraulis* and *Dryas*, using a coalescent-based approach that has been increasingly used in recent years (Yang, 2015; Matos-Maraví *et al.*, 2019; Núñez *et al.*, 2020). We also perform the first morphometric and wing pattern studies for taxonomic purposes within both genera.

Material and methods

Taxon sampling and molecular procedures

Of the eight recognized subspecies of *A. vanillae*, we obtained sequences of seven: *forbesi* Michener, 1942; *lucina* C. Felder & R. Felder, 1862; *incarnata* (Riley, 1926); *vanillae* (Linnaeus, 1758); *nigrior* Michener, 1942; *maculosa* (Stichel, 1908) and *insularis* Maynard, 1889 (Table S1). In addition, one undescribed taxon from Peru was also included referred from here on as *Agraulis* sp. We retrieved sequence data belonging to 9 of the 14 recognized *D. iulia* subspecies: *alcionea* (Cramer, 1779); *carteri* (Riley, 1926); *delila* (Fabricius, 1775); *dominicana* (Hall, 1917); *fucatus* (Boddaert, 1783); *iulia* (Fabricius, 1775); *martinica* Enrico & Pinchon, 1969; *moderata* (Riley, 1926) and *nudeola* (Bates, 1934). Representatives of other Heliconiini genera were also added to the dataset as outgroups for time divergence analyses to estimate the crown age of *Agraulis* and *Dryas* (Table S1).

DNA was extracted from leg tissues of dried specimens using the DNeasy kit (Qiagen, Hilden, Germany). We amplified and sequenced the following gene fragments for *Dryas* and *Agraulis* specimens, totalling 4199 bp: the mitochondrial genes 16S (518 bp) and cytochrome c oxidase subunit I (both its barcoding fragment, 658 bp and the following 841 bp fragment), and the nuclear genes apterous, 203 bp; elongation factor 1α,

795 bp; tyrosine hydroxylase, 736 bp and wingless, 447 bp (Table S1). We used primers and PCR protocols described in Sperling (2003), Kronforst (2005), Beltrán *et al.* (2007) and Massaro *et al.* (2014). Sequence assembling and editing were performed using SEQUENCHER 4.10.1 (Gene Codes, Ann Arbor, MI, U.S.A.).

Divergence time estimation and species delimitation

We applied the Bayesian Phylogenetics and Phylogeography (BPP) method to delimit *Agraulis* and *Dryas* species as implemented in BPP 3.4 software (Yang, 2015). The method uses the multi-species coalescent model (MSC) to compare different models of species delimitation and species phylogeny in a Bayesian framework.

Since BPP requires a priori assignment of the specimens to putative species, we first inferred a coalescent species-tree for each genus using all available specimens performing a STARBEAST analysis in BEAST 2.5.2 (Ogilvie *et al.*, 2017) without assigning specimens to species. A lognormal relaxed-clock model was applied to each locus (M = 0, S = 1) under a Yule tree prior and a linear with constant root population size model. We performed two independent MCMC runs, with each chain running for 100 million generations and trees and parameters sampled every 5000 generations. We assessed convergence of the analyses in TRACER 1.6 and sample size above 200 for each parameter and combined the sampled trees in LogCombiner discarding 25% of the trees. We constructed a maximum clade credibility tree in TREEANNOTATOR. Following the topology of the tree obtained for each genus (Figures S1, S2), and taking also into account the results of Davies & Bermingham (2002) and Runquist *et al.* (2012) as well as COI barcode divergence and geographic distribution, we assigned specimens to putative species in the BPP analyses.

We used STARBEAST2 (Ogilvie *et al.*, 2017) to infer calibrated species trees and estimate the divergence time of the root for each genus. Substitution models were inferred for each locus with PARTITIONFINDER v.0.1 (Lanfear *et al.*, 2012). We assigned to the mitochondrial loci a gene ploidy of 0.5 and 2.0 (diploid) to the nuclear ones. Uncorrelated relaxed–clock models were chosen for all loci, and we estimated nuclear clock rates relative to the COI mean clock rate fixed to 1.0. The relative clock mean priors were all log–normal (M = 0, S = 1). We ran five analyses for 100 million generations with sampling every 5000 generations with a pre burn in of 25 million generations. Since no Heliconiinae fossils are known, we used a secondary calibration at the root of the Heliconiini phylogeny of 23 Ma employing a uniform prior to constrain the root to 18–27 Ma, following the results from two recent studies that employed different taxon sets and methodologies and achieved similar estimates (Chazot *et al.*, 2019; Zhang *et al.*, 2019). Convergence among the runs, effective sample sizes and divergence times with upper and lower 95% HPD bounds were assessed in TRACER 1.6. The results of the runs were combined with LogCombiner after discarding 25% of the samples. TreeAnnotator was used to summarize the results with a 10% burn-in. The generated tree was visualized and edited in FIGTREE 1.4.3.

In our BPP analyses, the heredity scalar was set to 0.25 for the mitochondrial loci and to 1 for the nuclear. The programme uses inverse–gamma priors, IG (α, β), for the θs and τs parameters of the MSC model and for both, we used $\alpha = 3$ for a diffuse prior. β adds the information concerning genetic diversity, and we evaluated four different scenarios. Following the recommendations of Leache & Fujita (Leaché & Fujita, 2010), we set a conservative prior $\beta = 0.2$, or 2 changes per 1000 bp; an intermediate $\beta = 0.1$, or 1 change per 1000 bp and the least conservative $\beta = 0.02$, or 2 changes per 100 bp. For the fourth scenario, we measured the mean genetic diversity of our *Agraulis* and *Dryas* sequences, 0.0238 and 0.016, or 2.38 and 1.6 differences per 100 bp, respectively. Considering these values and that $\beta = \text{mean}*(\alpha-1)$ should be above 0.0476 and 0.032, respectively, we set $\beta = 0.08$ and 0.05, or 8 and 5 changes per 100 bp, respectively, as sensitive priors in the fourth analyses. For the prior distribution of $\tau\Theta$, the parameter controlling the divergence time of the root in the species trees, we specified $\beta = 0.0498$ and $\beta = 0.216$ enforcing a sequence divergence mean of 1.96 and 1.31%, which translates into absolute times of c. 8.59 and 3.73 Ma for the crown age of *Agraulis* and *Dryas*, respectively (Figure S3), assuming a mutation rate of 2.9×10^{-9} (Keightley *et al.*, 2015).

We performed an unguided species delimitation, BPP model A11, employing 500 000 generations with sampling every 50 generations and a burn–in of 10 000 generations. We ran the analysis twice using a different seed number for each combination of parameters to confirm the consistency of the results.

We also performed a total-evidence-based Bayesian approach for species delimitation combining the molecular dataset and morphometric data as implemented in IBPP 2.1.2 (Solis-Lemus *et al.*, 2015). We used three priors parameter combinations: $\theta = 1$ and $\tau = 10$, $\theta = 1$ and $\tau = 2000$ and $\theta = 2$ and $\tau = 2000$, and ran both the algorithms 0 and 1 with different values of ε and α and m, respectively, and different seed numbers. The landmarks that not contributed to the data variation, according to the principal components analysis (PCA) results (see below), were excluded. The analysis sometimes got stuck in a single species model, resulting in poor overall convergence.

We compared the different species hypotheses by comparing their marginal likelihood estimates (MLE) using path sampling (Baele *et al.*, 2013) in BEAST 2.5.2 (Bouckaert *et al.*, 2014). We used 50 steps with chains running for 100 000 generations with sampling every 10 000 cycles. We always checked that the final ESS values were above 200. The support for the species delimitation hypotheses was assessed via Bayes factors (Kass & Raftery, 1995).

COI barcodes

We gathered all available COI barcodes from GenBank and BOLD and produced 64 additional sequences that were submitted to the aforementioned repository (Table S2). In total, we analysed 79 barcodes of *Agraulis* and 95 of *Dryas*. We

calculated p-distances among all available barcode sequences and also among and within the groups defined by the molecular species delimitation analyses. Calculations were performed using MEGA 7 (Kumar *et al.*, 2016). We constructed a Neighbor-Net haplotype network for each genus using SPLITSTREE 4.14.8 (Huson & Bryant, 2006) and represented geographically the haplotypes employing popart 1.7 (Leigh & Bryant, 2015). We also employed a character-based approach looking for diagnostic positions in the barcode sequences of each species. We inspected the sequences visually, after extracting the informative sites in MEGA, and annotated the diagnostic characters or combination of characters for individual taxa or groups of taxa. For positions that varied within a taxon, we only took those exhibiting one state, or nucleotide, in 90% of the samples. Variable positions below that threshold were discarded.

Dryas *allozyme data*

Davies & Bermingham's (2002) historical biogeography study included one of the largest samples for any butterfly species in the West Indies to date. They sampled 249 specimens covering all *D. iulia* subspecies except *zoe* Miller & Steinhauser, 1992 from the Cayman Islands. Unfortunately, their sequence data for COI–COII and allozymes are not publicly available. However, we captured the allelic frequencies for 17 loci from their Appendix II and performed a hierarchical clustering analysis in PAST 4.02 (Hammer *et al.*, 2001). We used both Ward's method and UPGMA algorithms using Euclidean and Bray–Curtis similarity indices, respectively, and ran 1000 bootstrap replicates each time.

Morphometrics

We examined adult specimens deposited at the Zoologische Staatssammlung München, ZSM (Munich, Germany), the McGuire Centre for Lepidoptera and Biodiversity, Florida Museum of Natural History (Gainesville, FL, U.S.A.), the Víctor González Research Collection (San Juan, Puerto Rico) and the Institute of Ecology and Systematics (Havana, Cuba). We analysed photographs taken with a Nikon D5100 camera of 192 specimens of *Agraulis* and 224 of *Dryas* (Table 1). We grouped the subspecific taxa into the species resulting from the molecular species delimitation analyses. In *Agraulis*, *A. v. galapagensis* specimens, absent from the molecular analyses, were added as group. Since *D. iulia* subspecies *largo*, *framptoni*, *lucia* and *warneri* were absent from our molecular sampling, we assigned them to each hypothetical species following the results from Davies & Bermingham (2002). We assigned *zoe*, which is absent from any molecular studies, based on its external appearance and geographic distribution.

Linear measurements. We measured the right forewing and right hindwing lengths (FWL, HWL) of each specimen, taken as the distance from wing base to apex using landmarks 1–9 and 1–14 (see below), respectively, using IMAGEJ (Rasband, 2007).

Table 1. Specimens per taxon included in the morphometric study of *Agraulis* and *Dryas*.

Agraulis			*Dryas*		
Taxa	Males	Females	Taxa	Males	Females
Agraulis sp.	2	1	*D. i. alcionea*	62	5
A. v. forbesi	16	6	*D. i. carteri*	3	2
A. v. galapagensis	2	3	*D. i. delila*	9	9
A. v. incarnata	20	16	*D. i. dominicana*	4	3
A. v. insularis	16	13	*D. i. framptoni*	2	1
A. v. lucina	15	1	*D. i. fucatus*	13	6
A. v. maculosa	21	20	*D. i. iulia*	3	-
A. v. nigrior	13	6	*D. i. largo*	11	8
A. v. vanillae	11	10	*D. i. lucia*	6	1
			D. i. martinica	4	2
			D. i. moderata	42	3
			D. i. nudeola	9	8
			D. i. warneri	4	-
			D. i. zoe	2	2
Total: 192	116	76	Total: 224	174	50

Before the comparisons of linear measurements, we performed a Monte Carlo test that detected no differences in FWL and HWL between sexes, thus we used males and females together in these comparisons. However, we did detect differences in the wing aspect ratio, HWL–FWL, between sexes of the same taxon. We compared FWL and HWL between groups and aspect ratio between groups by sex through PERMANOVA tests using Euclidean distance as a measure of distance and performing 10 000 permutations. Aspect ratio between sexes of the same taxon was compared by an unpaired *t*-test or a Mann–Whitney Test in absence of normality, or when there were too few values. All tests were performed in PAST 4.02 (Hammer *et al.*, 2001).

Landmark-based wing shape comparisons. We compared the shape of both wings among groups using a landmark-based approach. Landmarks were placed at the origin and end of veins in a distribution that can be used as a proxy of shape. These points meet the criteria of Zelditch *et al.* (2012) for landmark selection, being easy to identify, morphologically significant, lying in the same plane, conserved in all individuals and providing an adequate coverage of the morphological structure to be quantified. Landmarks at the origin and end of veins have been commonly used in morphometric studies on insects (Dworkin & Gibson, 2006; Breuker *et al.*, 2010; Bai *et al.*, 2016; Goonesekera *et al.*, 2018). We digitized 17 landmarks on the forewing (FW) on specimens of both genera (Figure S4) using TPSDIG v. 2. (Rohlf, 2006). On the hindwing (HW), 13 landmarks were placed on *Agraulis* specimens and 16 on those belonging to *Dryas* (Figure S4). On the *Dryas* HW, we focused on the outer margin since we noted differences a priori between populations. The landmark coordinates obtained both genera are available as .DAT files, PAST format, in the Appendices S1 and S2.

Landmark coordinates were superimposed with a generalized least-squares Procrustes method (Dryden & Mardia, 1998) in PAST 4.02. This procedure allows the removal of the effects of translation, scaling and rotation on shape. To assess the contribution of each landmark to the variability of the dataset,

we performed a PCA of landmark coordinates, or relative warp analysis (Bookstein, 1989). We also employed thin-plate splines (TPS) deformation grids (Dryden & Mardia, 1998) to represent the variability of wing shape explained by each principal component (PC). TPS was also used to visualize shape change between sexes and among groups. All analyses were performed in PAST 4.02.

The percentage of anisotropy, or the extent of shape deformation with respect to a reference form, was calculated for the wings of each taxon as the sum of the deformations of all landmarks. We followed Bookstein (1989) and calculated this percentage at each landmark as $((1 + S1)/(1 + S2) - 1) \times 100$, where $S1$ and $S2$ are the two principal strains. We used the R package phytools (Revell, 2012) to visualize the evolution of wing shape traits across the phylogeny for each genus.

We tested if FW and HW shape differed among groups by comparing the Procrustes distances, both for males and females, performing 10 000 permutations. We ran the tests in MORPHOJ (Klingenberg, 2011).

We performed discriminant analyses to test if the specimens of each group can be classified using the information of the landmarks from each wing, and also combined after the Procrustes superimposition procedure of each wing. Since our dataset does not meet all assumptions of the Linear Discriminant Analysis, we performed flexible discriminant analyses (FDA) (Hastie *et al.*, 1994) using the R package mda (Leisch *et al.*, 2020). We implemented the three available methods: polyreg, MARS and BRUTO.

Forewing colour pattern analyses

We analysed the dorsal FW black spot pattern of *Agraulis* and *Dryas* using the R package *patternize* (Van Belleghem *et al.*, 2017). We aligned right FW images through automatic image registration, extracted the black colour pattern from the images using an RGB threshold procedure and performed a PCA with the resulting data. The analyses were performed independently for each sex since both *Agraulis* and *Dryas* exhibit sexual dimorphism related to the extension of the black spot pattern on the FW.

Comparison of the colour pattern in Dryas *mature larvae*

We examined all available data of *Dryas* mature larvae after preliminary observations revealed distinct features among different populations. We photographed or reared larvae of several *Dryas* subspecies using *Passiflora* spp. as host plants: *D. iulia alcionea* (Surinam, French Guiana), *D. iulia moderata* (Costa Rica), *D. iulia delila* (Jamaica), *D. iulia nudeola* (Cuba), *D. iulia iulia* (Puerto Rico), *D. iulia fucatus* (Dominican Republic), *D. iulia dominicana* (Guadeloupe) and *D. iulia martinica* (Martinique).

We searched for descriptions and illustrations of mature larvae in the literature, finding information on the following taxa: *D. iulia alcionea* (Beebe *et al.*, 1960; Paim *et al.*, 2004; da Silva

et al., 2006), *D. iulia largo* (Minno & Emmel, 1993), *D. iulia martinica* (David & Lucas, 2017) and *D. iulia zoe* (Askew & Stafford, 2008). We also examined photographs with locality information at the Butterflies of America (Warren *et al.*, 2017) and Área de Conservación de Guanacaste websites (janzen.sas.upenn.edu/caterpillars/database.lasso).

Geographic distribution

We compiled our field data, the data of the specimens from the morphometric study (see above at Section 2.3), and specimen data from collections at the Museo de Historia Natural Universidad Nacional Mayor de San Marcos, Lima, the Museo de Historia Natural Noel Kempff Mercado, Santa Cruz, the Colección Boliviana de Fauna, La Paz, the Centro de Biodiversidad y Genética, Cochabamba, the Universidad Técnica Particular de Loja, Loja, the Instituto Nacional de Biodiversidad, Quito, the Museo de Historia Natural Alcide d'Orbigny, Cochabamba, the Staatliches Museum für Naturkunde, Stuttgart and the Florida Museum of Natural History, Gainesville (Table S3). Finally, we also retrieved data available from the online database of the Museum of Comparative Zoology (MCZ), Harvard (http://mczbase.harvard.edu/), where we carefully checked the identity of each specimen before using their images.

Results

Coalescent based species delimitation

Our BPP analyses using the four combinations of priors yielded three different species hypothesis for *Agraulis* and two for *Dryas* (Fig. 1). The iBPP analyses using the molecular dataset combined with wing measurements and landmarks yielded two species hypotheses for *Agraulis* and three for *Dryas* matching the BPP results except for one additional hypothesis for *Dryas* (asterisks in Fig. 1, Tables S4, S5). There was no variation in the results of the BPP runs with identical prior parameters for both genera and in the iBPP runs for *Agraulis* regardless of the prior combination used. The iBPP analyses of *Dryas* yielded the same three hypotheses in several runs with each prior combination (Tables S4, S5). In our hypothesis-testing runs, we also included the current traditional taxonomy, namely a single species in each genus. The hypotheses with seven and four species for *Agraulis* and *Dryas*, respectively, scored the highest MLE (Table 2). *Agraulis* eight putative species, *A. v. galapagensis*, was absent from our analyses. Support for all these hypothetical species was strong with posterior probabilities above 0.94, except for the hypotheses involving *A. vanillae nigrior* and *A. vanillae incarnata* (Fig. 1). MLE differences of the favoured hypotheses with respect to others were well above 10, which is considered decisive support for the hypothesis with the highest score (Table 2). There is one exception in *Agraulis*, where the eight species hypothesis scored only 0.2 units below the best one. We prefer the more conservative seven species hypothesis for *Agraulis* with *nigrior* included
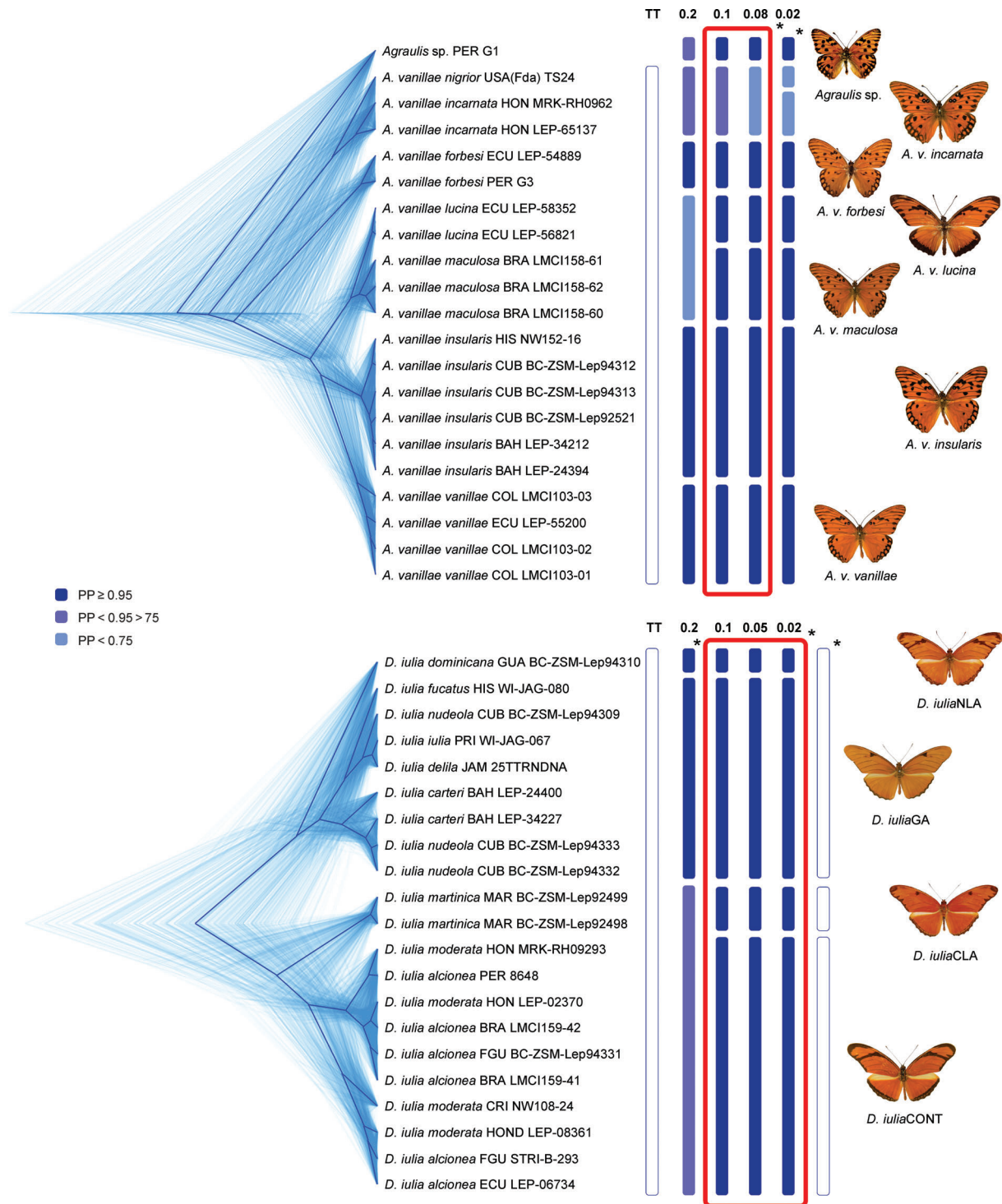
Fig. 1. Species delimitation hypotheses for *Agraulis* and *Dryas* obtained in Bayesian Phylogenetics and Phylogeography (BPP) and iBPP. Species tree generated in STARBEAST using six markers: 16S, COI, wingless, apterous, TH and EF1a. Values used for the β prior of the θs parameter of BPP: 0.2 – highly conservative, 0.1 – intermediate, 0.02 – least conservative and 0.08 and 0.05 based on the genetic diversity of the *Agraulis* and *Dryas* datasets, respectively. Solid bars represent analyses output with posterior probabilities for each species hypothesis obtained in BPP as shown in legend. The asterisks represent the species hypotheses from iBPP, see text and Tables S4, S5 for details on priors and species posterior probabilities. The empty bars represent the traditional taxonomy (TT), a single species on each genus, and another hypothesis for *Dryas* obtained in iBPP. Cloudograms are based on 500 posterior trees from the coalescent species tree analyses in BEAST, the thicker blue line represents the consensus tree. The favoured hypotheses, based on Bayes factors (Table 2), are demarcated by a thick red empty bar.

Table 2. Marginal likelihood estimate (MLE) values using path sampling for each species hypothesis for *Agraulis* and *Dryas* from the BPP and iBPP analyses and the traditional taxonomy, TT.

Species hypotheses	Theta prior(s)/iBPP*	MLE	Ln BF
Agraulis			
1 species	-/TT	−9413.6	100.1
6 species	0.2	−9354.5	41
7 species	0.1/0.08/iBPP	−9313.5	-
8 species	0.02/iBPP	−9313.7	0.2
Dryas			
1 species	-/TT	−10441.1	95.3
3 species A	0.2/iBPP	−10390.7	44.9
3 species B	iBPP	−10380.6	34.8
4 species	0.1/0.05/0.02/iBPP	−10345.8	-

Log Bayes factor, ln Bf, values from 2 to 10 represent positive but not conclusive support and >10 represent decisive support for the hypothesis with the highest MLE. Several priors together indicate the same species hypothesis output. *Dryas* three hypotheses correspond to *D. iulia*CONT + *D. iulia*CLA, *D. iulia*NLA, *D. iulia*GA (A) and to *D. iulia*CONT, *D. iulia*CLA, *D. iulia*NLA + *D. iulia*GA (B). See Tables S4, S5 for details on iBPP priors and output.

within *incarnata*. All species were recovered as monophyletic in the coalescent tree reconstructed prior to the BPP analyses (Figures S1, S2). Only in some of the trees recovered with the mitochondrial and nuclear datasets separated some mixing occurred among specimens of species of very recent origin, *for example*, *D. iulia*NLA and *D. iulia*GA and *A. v. lucina* and *A. v. maculosa* (Figures S5, S6), with support weak in most shallow nodes. The traditional single-species hypothesis scored worst in both genera. The *Agraulis* species almost perfectly matched the currently recognized subspecies and are mentioned likewise from now on, except for *nigrior*, which is included within *A. v. incarnata*. In the case of *Dryas*, we provisionally named the species: *D. iulia*CONT (both continental subspecies and south Lesser Antilles *framptoni*), *D. iulia*CLA (central Lesser Antilles *lucia* and *martinica*), *D. iulia*NLA (northern Lesser Antilles, *dominicana* and *warneri*) and *D. iulia*GA (all subspecies from the Greater Antilles, Bahamas, Cayman Islands and south Florida, U.S.A.).

COI barcode analysis

Simple p-distances among COI barcode sequences belonging to *Agraulis* and *Dryas* specimens ranged from 0 to 6.18% and 3.61%, respectively. Average distance among species was from 1.09 to 5.81% in *Agraulis* and from 1.09 to 3.44% in *Dryas* (Table 3). Minimum distance among specimens assigned to different species hypotheses was 0.55 between *A. v. insularis* and *A. v. maculosa* (Table 3). Within-group distances ranged from 0 to 1.11% in *Agraulis* and from 0 to 2.43% in *Dryas*.

The NeighborNet haplotype network shows a well-structured net for *Agraulis* sequences (Fig. 2). There is a dichotomy between *D. iulia*GA and the single *D. iulia*NLA sequence. Both *D. iulia*CLA sequences appear on a long branch nested within *D. iulia*CONT (Fig. 2). The highest within-group variability occurs in *D. iulia*CONT with two sequences differing up to 1.98 (JN308883) and 2.43% (GU678536) from sequences of their own group. However, these two sequences also differ from sequences of the other three groups starting in 1.72 and 2.03%, respectively.

The plotting of haplotypes on a map shows that, both in *Agraulis* and *Dryas*, haplotypes are only found within each species hypothesis, regardless of whether the localities are nearby or widely separated or if they are separated by land or sea (Fig. 2). We recovered several haplotypes of *A. v. insularis* and *D. iulia*GA widespread across the Bahamas (several islands), Cuba, Jamaica, Hispaniola, Puerto Rico and Culebra Island at the Greater Antilles (Fig. 2). A private sequence at BOLD from the Florida Keys, subspecies *largo*, matches one *D. iulia*GA haplotype from Cuba and the Bahamas. Haplotypes from Guadeloupe, *D. iulia*NLA, and Martinique, *D. iulia*CLA, are exclusive to these territories. On the continent there are two *D. iulia*CONT haplotypes distributed from the Yucatán Peninsula southward to northern Argentina (Fig. 2). All South American haplotypes of *D. iulia*CONT to the west of the Andes cordillera are shared with Central America.

The character-based approach found exclusive diagnostic positions for all *Agraulis* groups except *A. v. maculosa* (Table S6). However, the latter still can be recognized by a

Table 3. Mean p-distances among COI sequences of species hypotheses within *Agraulis* and *Dryas*, bottom left.

	Agraulis sp.	*A. v. forbesi*	*A. v. incarnata*	*A. v. insularis*	*A. v. lucina*	*A. v. maculosa*	*A. v. vanillae*
Agraulis sp. (n = 1)	-	5.69	4.98	4.74	3.85	4.5	5.48
A. v. forbesi (n = 4)	5.81	**0.32**	3.81	3.14	3.14	2.77	3.92
A. v. incarnata (n = 20)	5.15	4.01	**0.14**	2.77	2.94	2.21	2.99
A. v. insularis (n = 23)	4.91	3.38	2.93	**0.25**	1.11	0.55	1.31
A. v. lucina (n = 4)	3.99	3.29	3.01	1.42	**0.16**	0.74	1.87
A. v. maculosa (n = 18)	4.65	2.92	2.73	1.23	1.09	**0.38**	1.49
A. v. vanillae (n = 5)	5.65	3.8	3.00	1.5	2.04	1.89	**0.11**

	*D. iulia*CONT	*D. iulia*CLA	*D. iulia*NLA	*D. iulia*GA
*D. iulia*CONT (n = 72)	**0.56**	1.25	1.49	1.41
*D. iulia*CLA (n = 2)	1.86	**0.00**	3.44	2.82
*D. iulia*NLA (n = 1)	2.22	3.44	-	0.82
*D. iulia*GA (n = 18)	1.95	3.01	1.07	**0.19**

Minimum p-distances between species hypotheses, upper right. Sample size is given within brackets and within group average distance is shown in bold.
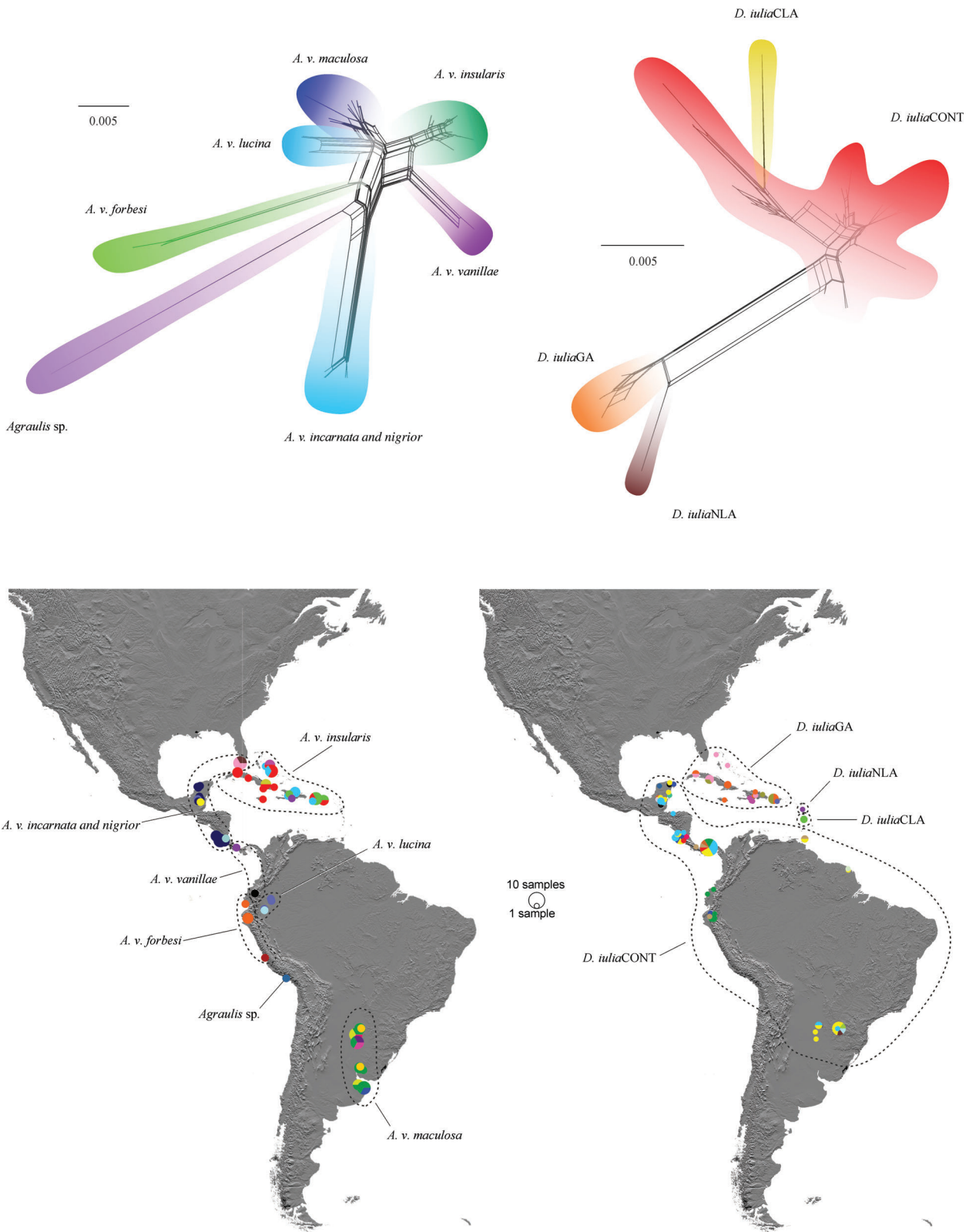
Fig. 2. NeighborNet networks obtained in SplitsTree and geographic distribution of the haplotypes present in 79 and 95 COI barcode sequences of *Agraulis* and *Dryas*, respectively. Colours in the networks represent the species hypotheses and in the maps different haplotypes. There are no haplotypes shared among species hypotheses. Dashed lines demarcating each species hypothesis.

unique combination of the 44 nucleotide positions analysed. There is even a position, 283, allowing the separation of the two subspecies we included within *A. v. incarnata* for the analysis. Regarding *Dryas*, exclusive positions were only found in *D. iulia*NLA and *D. iulia*CLA (Table S6). These two groups differ by four and six positions from their closest relatives, *D. iulia*GA and *D. iulia*CONT, respectively. All specimens of both members of these two pairs also differ in six other positions from all members of the other pair (Table S6). The two highly different sequences of *D. iulia*CONT mentioned above share the same diagnostic positions with the rest of their group.

Dryas *allozyme data revisited*

The hierarchical clustering of the 17 allozyme allelic frequencies yielded identical trees dividing *Dryas* into two main clusters, with each divided into two smaller ones (Figure S7, only one method is shown). One of the main clusters contains *D. i. lucia* and *D. i. martinica* (*D. iulia*CLA), joined to the other subcluster containing the specimens of the southernmost Lesser Antilles subspecies, *D. i. framptoni*, and the continental *D. i. alcionea* and *D. i. moderata* (*D. iulia*CONT). The other main cluster contains *D. i. dominicana* and *D. i. warneri* (*D. iulia*NLA) separated from a larger subcluster (*D. iulia*GA) grouping all Greater Antillean, Bahaman and South Florida taxa. Bootstrap values for the major groups and deeper nodes were 70 or higher in both methods (Figure S7).

Morphometrics

Linear measurements. *Agraulis*. Mean FWL differed among species (Figure S8, Table S7). *Agraulis v. galapagensis* and *Agraulis* sp. are similar in size but smaller than all other taxa. Measurements of *A. v. forbesi*, *A. v. vanillae* and *A. v. incarnata* had large confidence intervals. *Agraulis v. lucina* was the largest taxon and *A. v. insularis* was the least variable, differing both from their sister taxa *A. v. maculosa* and *A. v. vanillae*, respectively. HWL differed among taxa but the differences were less marked than in FWL (Figure S8, Table S7). *Agraulis v. galapagensis* was again different from all other taxa except *Agraulis* sp.

Wing aspect ratio for each sex differed among some taxa and between sexes of the same taxon, with females having proportionally larger HW compared to males (Figure S8, Table S7). Only *A. v. vanillae* was not different from most other taxa. *Agraulis v. galapagensis* and *Agraulis* sp. were not different from one another. Among females the differences were less marked than among males, only *A. v. forbesi* and *A. v galapagensis* were different from most other taxa but not from one another. *Agraulis* sp. and *A. v. lucina* exhibited the highest and lowest aspect ratio, respectively. Due to the low sample size for females of some taxa, the output of the aspect ratio permutations test might be misleading.

Dryas. FWL and HWL differ among the four hypothetical species (Figure S8, Table S8). For both measurements, *D. iulia*NLA was not different from *D. iulia*CONT and *D.*

*iulia*CLA, with all other taxa different from one another. Wing aspect ratio was also different among males and females except in *D. iulia*CLA (Figure S8, Table S8). In males, *D. iulia*NLA was not different from *D. iulia*GA and *D. iulia*CLA, while the latter was not different from *D. iulia*CONT. In females, results were similar but *D. iulia*CLA was not different from *D. iulia*GA.

PCAs of landmark coordinates. The PCA of landmarks coordinates of *Agraulis* and *Dryas* FW and HW described between 38.8 and 63.7% of variability in the first two PCs, respectively (Figs 3, 4). Though eigenvectors showed that 11–16 PCs are needed to express 95% of the total variation (Tables S9, S10), only the first two to five are meaningful according to the broken stick model (Figure S9).

Agraulis. On the FW, PC1 shows that landmarks 1 and 16, which correspond to the wing base and the origin of the Cu1 vein, respectively, contribute the most to the total variability (Fig. 3, Table S9). The displacement of landmarks 16 and 17 in this PC translates into compression and expansion of the middle and distal portions of the cell, respectively, and is a clear evidence of sexual dimorphism. In males, the Cu1 vein origin is much closer to the end of the cell (min PC1 in Fig. 3) whereas in females it is closer to the middle of the cell (max PC1 in Fig. 3). In FW PC2 the variability is more distributed, landmarks with the greater contribution are related with the tornus, the end of veins A1 + 2 and Cu2, landmarks 2 and 3, the wing, 9 and 10, and cell, 13 and 14, apices and again the origin of the vein Cu1 (Fig. 3, Table S9). In PC2, the distal portion of the cell is compressed and its middle portion is expanded, 14–16, and there is an outward displacement of the wing apex, 9–10, and the tornus, 2–4.

In the PC1 of *Agraulis* HW most of the variability lies on the end of veins Cu2, landmark 4, M1, 8, and Sc + R1, 9 and at the origin of Cu2, 13 (Fig. 3). Deformations involve compression at the tornus, 3–5, the expansion of the apex, 8–9 and an enlargement of the cell, 10–13 (Fig. 3). At HW PC2 the landmarks related with the end of veins A3, 2, Cu1, 5 and Sc + R1 show greater variability (Fig. 3, Table S9). Deformation in PC2 translates in a shorter A3 vein, 2 and a broader outer margin, 4–5 and 8–9.

Dryas. In FW PC1, the landmarks contributing the most to the total variability are related with the base, 1, the end of veins A1 + 2 and Cu2 at the tornus, 2–3 and vein R4 at the apex, 10 (Fig. 4, Table S10). Deformation in PC1 involves a narrower tornus, 2–4, a shorter branching of the radial system, 10–12, and an enlarged cell apex, 13–14. Variability in PC2 is related to landmarks 1 and 10 again, but also 4 and 5, the end of veins Cu1 and M3, respectively. Deformation at FW PC2 is related with a more concave middle portion of the outer margin, 3–6, and an expanded wing apex, 8–9. On the HW, variability at PC1 was mostly related with the base, 1 and landmarks on the outer margin, 6 and 13–14, with deformation implying compression on the middle portion and expansion of the outer margin producing a more crenulate outline. Most variability at HW PC2 lies in the base and cell landmarks, 1 and 15–16, respectively, and at the wing apex, 13–14, with deformation,
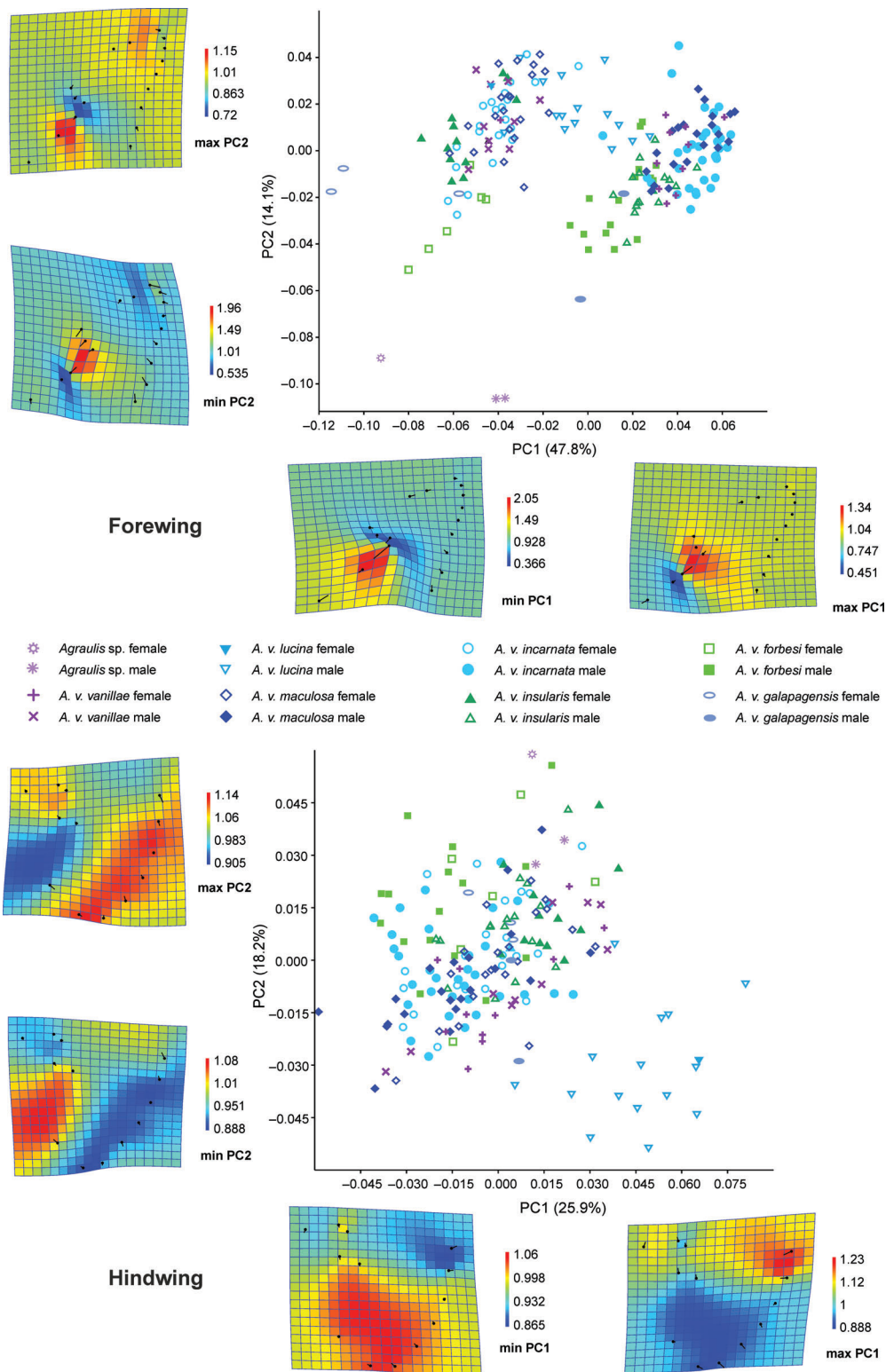
Fig. 3. Principal Components Analyses of landmarks of the both wings of *Agraulis*. Heatmaps representing the landmarks displacement on the extremes of each principal component (PC). The extremes of the colour scales represent shape expansion (higher values) or compression (lower values). See Figure S9 and Table S9 for information on the meaningful PCs and the contribution of each landmark to the total variability, respectively.
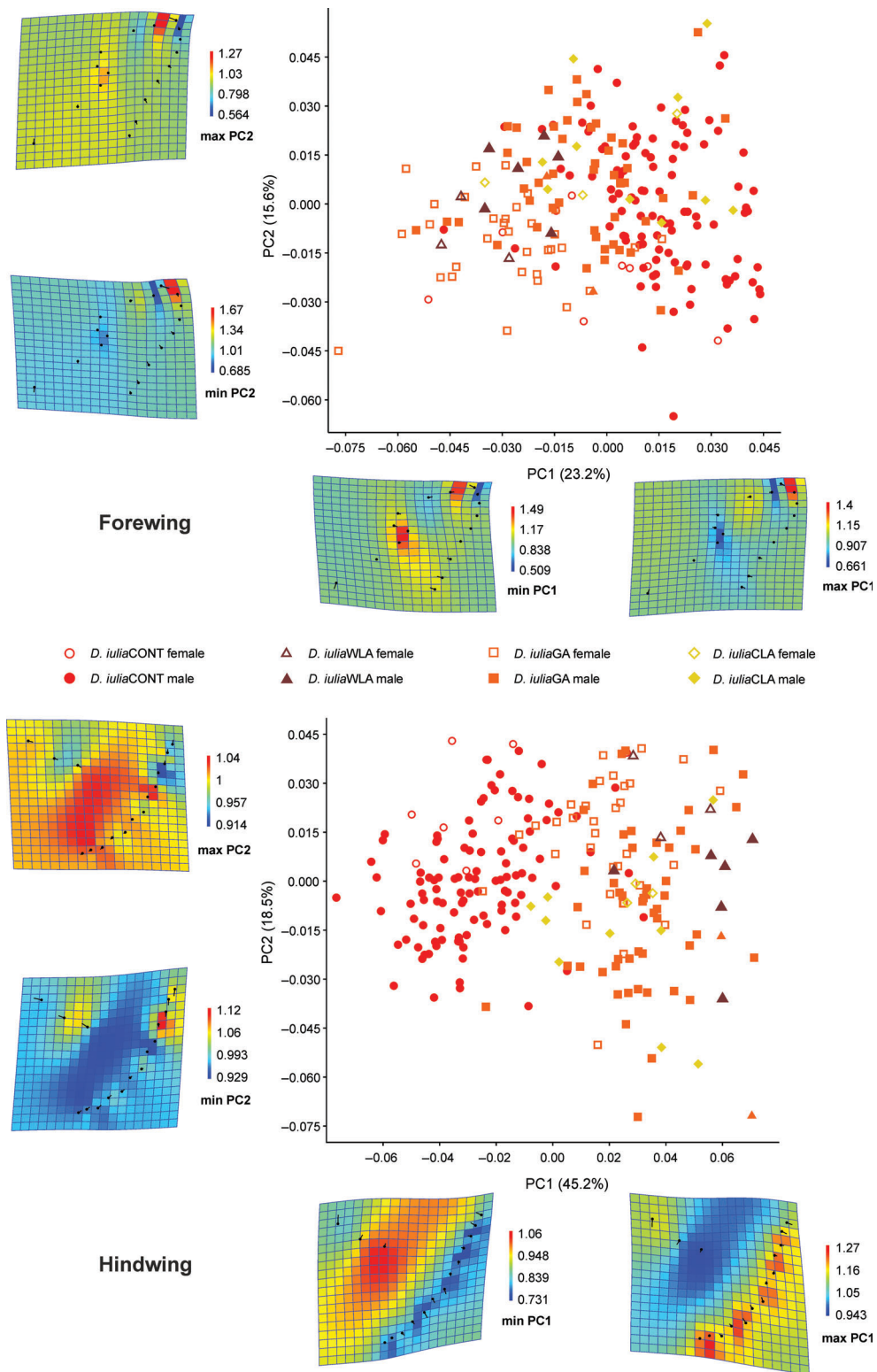
Fig. 4. Principal Components Analyses of landmarks of the both wings of *Dryas*. Heatmaps representing the landmarks displacement on the extremes of each principal component (PC). The extremes of the colour scales represent shape expansion (higher values) or compression (lower values). See Figure S9 and Table S10 for information on the meaningful PCs and the contribution of each landmark to the total variability, respectively.

including the outward expansion of the distal half of wing and a narrower outer margin (Fig. 4, Table S10).

TPS deformation grids. *Agraulis.* Overall FW deformation implies that males have a broader wing compared to females. This is due to the displacement of the wing base and the veins ending at the tornus, landmarks 1–4 (Figs 3, S10). As noted above, in males the origin of the Cu1 vein, landmark 16, is much closer to the end of cell whereas in females it is near the middle (Fig. 3). This trend is also present in each taxon when analysed separately (Figure S11A). On the HW, sexual dimorphism is almost indistinct: origins of Sc + Rs and M1, landmarks 10 and 11, are slightly more separated in males, which also have a slightly narrower HW due to compression (Fig. 3). Other signs of sexual dimorphism are males having a shorter radial system, landmarks 11 and 12 and a broader HW due to a more pronounced tornus, 2–4 (Fig. 3, S10, S11A).

TPS grids proved to be useful to visualize how wing shape changes in each taxon with respect to a mean shape estimated for the genus and how shape changes between pairs of taxa (Figures S11B, C, S12). There is a high extent of deformation between the closely related *A. v. maculosa* and *A. v. lucina*, the latter having a much more slender FW and an HW with a larger cell, an expanded apex and a compressed tornus (Figure S12). Mean shape change from *Agraulis* sp. to its geographical neighbour, *A. v. forbesi*, implies a narrowed FW, a proportionally shorter FW cell with more separated Cu veins and the origin of the HW Cu veins more separated (Figure S12).

Dryas. Sexual dimorphism in wing shape is also present in *Dryas* but is less evident (Figure S10). Deformation of genus mean shape from female to male includes a shortening of the radial system, landmarks 11–12 and a more concave middle portion on the FW outer margin, 4–5 (Figure S10). On the HW, the origins of the Cu veins are more separated, 15–16. The compression along the outer margin and the displacements on tornus and apex implies that males possess a narrower FW and a broader HW. Several of these trends are also appreciable within each taxon (Figure S13A).

TPS grids show that *D. iulia*CONT possesses an FW with broader apex, 9–10, and the Cu1 origin closer to the cell end, 14–15, while its HW is expanded in the discal cell and it has a less crenulate outer margin, 2–14, with respect to the mean reference form (Figure S13B). The opposite of these trends occurs in *D. iulia*GA and in *D. iulia*NLA (Figure S13B).

Differences among the species include deformations toward a narrower apex and an expanded apical portion of the cell FW. In males, there is compression at the basal half of the HW of *D. iulia*CONT and *D. iulia*GA compared to *D. iulia*CLA and *D. iulia*NLA, respectively (Figure S12). A similar deformation in the FW is observed when comparing the mean shape of females *D. iulia*CONT against *D. iulia*GA, while the landmarks on the HW outer margin change towards a more crenulated margin (Figure S12).

Statistical comparison of the shape. *Agraulis.* Procrustes distances' permutations test for the FW shape detected significant

differences among all species (Table S11). For males, distances among all taxa differed in both the FW and HW except *A. v. galapagensis*, which did not differ from *A. v. forbesi* and *Agraulis* sp. For females, all taxa differed in FW shape except *A. v. lucina*, which was only different from *A. v. maculosa*, although this result was probably caused by the single female available for the former taxon (Table S11). *Agraulis v. maculosa* did not differ from *A. v. vanillae*. For the HW differences were less marked with *A. v. forbesi*, *A. v. galapagensis* and *Agraulis* sp. being similar to most other populations.

Dryas. Procrustes distances' permutations test found most hypothetical species to be different from each other, for both sexes and wings (Table S12). However, in the case of female *D. iulia*NLA, the HW was not different from *D. iulia*GA and *D. iulia*CLA, which also did not differ from one another (Table S12).

Shape change across the phylogeny. *Agraulis.* The extent of shape change with respect to a mean reference form has its maximum expression in both sexes of *Agraulis* sp. when analysing each wing separately and together (Figure S14, Table S13). The amount of shape change becomes smaller from the earliest to the most recently diverged taxa. However, there is a noteworthy exception; *A. v. lucina*, one of the most recently diverged taxa, exhibits the second-largest amount of change. Shape has changed in a more or less similar degree on both FW and HW, for example, *Agraulis* sp. males, *A. v. insularis* and *A. v. maculosa*, but can differ between wings, including between the sexes of the same taxon (Figure S14, Table S13). With respect to the mean form, the extent of change is higher on FW than on HW in *A. v. incarnata* males, whereas it is the opposite in females. The opposite case occurs in *A. v. forbesi* and *A. v. vanillae* (Figure S14, Table S13).

The amount of change between sexes of the same taxon, a proxy of sexual dimorphism in wing shape, decreases gradually, starting from the earliest diverging taxa (Figure S14). However, the extent of change increases again in *A. v. insularis* and *A. v. maculosa*, two of the most recently diverged taxa. The way in which sexual dimorphism in wing shape has evolved varies across the taxa. There is a higher extent of change on the FW between sexes in most taxa; however, shape change is higher on the HW than on the FW in *Agraulis* sp. and *A. v. lucina* (Figure S14, Table S13).

Dryas. The change of shape with respect to a mean reference form is highest in both sexes of *D. iulia*CONT followed by *D. iulia*NLA in the other clade (Figure S14, Table S14). Shape has changed to a more or less similar degree on both FW and HW in both sexes of *D. iulia*GA, which exhibits the smaller amount of change, and in *D. iulia*CLA females. Change with respect to the mean form of each wing is higher in FW than in HW in both sexes of *D. iulia*NLA and in *D. iulia*CLA males. HW shape has changed more than the FW in both sexes of *D. iulia*CONT (Figure S14, Table S14).

Sexual dimorphism in wing shape is lowest in *D. iulia*GA, with a similar amount of change in both wings (Figure S14). One member of each pair of taxa shows higher dimorphism

than its sister taxon. Shape change between sexes is expressed differently in each taxon. Besides how it occurs in *D. iulia*GA, mentioned above, the FW has changed more than HW with respect to the mean form of each wing in *D. iulia*CLA, whereas the opposite case occurs in its sister taxon *D. iulia*CONT. HW shape has changed more than the FW shape also in *D. iulia*NLA (Figure S14, Table S14).

Discriminant Analysis. *Agraulis*. As in the PCA analysis, the FDA plot of all *Agraulis* specimens in the analyses with FW and the FW and HW landmarks combined showed a split into two major groups, males and females (Fig. 5a, only the combined analysis is shown). After the removal of the two most distinct entities, *Agraulis* sp. and *A. v. lucina*, we ran two additional analyses: males and females of the remaining taxa separated (Fig. 5b). Percentages of correct classification of the specimens ranged from 84 to 100% depending on the sex, the method and the data used: each wing separately or combined (Table 7). Classification percentages did not change when the two most distinct entities were removed.

Dryas. The FDA plot of the eight groups, the four species separated by sex, shows a clear separation among them (Fig. 6, only the FW and HW combined analysis is shown). Data of FW landmarks correctly classified all specimens (Table 7). In terms of correctly classifying specimens, HW data scored between 68.8%, for females with the MARS method and 94.8%, for males with the polyreg method (Table 7). Classifying scores for the combined data ranged from 93.8 to 98.9% (Table 7).

Forewing pattern analysis. *Agraulis*. The FW pattern of *Agraulis* is best characterized as an orange background with dispersed black spots in the discal and post-discal areas (Figs 7, S4, S15). Sexual dimorphism includes the possession of modified androconial black scaling on veins in males and an extra spot on cell at the origin of Cu1 and additional submarginal spots centred on the veins in females (Figure S15). The only exception is *A. v. lucina*, where all but one of the discal spots are fused, the post-discal spots are missing, there is black along the costa and in the apex, and the additional spots are marginal and present in both sexes.

The first two PCs of the PCA for the spot pattern of FW explained 23.5 and 19.3% of variability in males and females, respectively (Fig. 7). *Agraulis v. lucina*, *A. v. galapagensis* and *Agraulis* sp. appear distant from the rest and there is little or no overlap among *A. v. maculosa*, *A. v. insularis* and *A. v. forbesi*. *Agraulis v. vanillae* overlaps with *A. v. forbesi* and *A. v. incarnata* with *A. v. maculosa* and *A. v. insularis* (Fig. 7). The extremes of the first two PC axes indicate that most important elements contributing to variability are the spots along margin, the absence of post-discal spots, the displacement and/or fusion of discal spots and the amount of black along veins. There was more overlap among females, although here the sampling is very small for some taxa. Elements contributing to the variability on the first two PC axes are the same as in males, but also include the possession or absence of the submarginal and the Cu1 spots and the displacement of the post-discal spots.

Dryas. The FW pattern of *Dryas* is characterized by an orange background with black bands along the anterior and outer margins and a band connecting their middle portion crossing the cell (Figs 7, S1, S15). Variability across the different taxa includes the reduction down to an almost entirely orange wing with thin black margins. Females of most taxa bear a complete or incomplete dark arched band, following the anal vein, from the base to the tornus.

The PCA for FW spot pattern explains 40.6% of variability in the first two PCs in males and 52.5% in females (Fig. 7). Among males, *D. iulia*CONT and *D. iulia*GA specimens overlapped only at one extreme of their distribution. However, *D. iulia*NLA and *D. iulia*CLA overlapped with the rest. For females, results were similar but the separation among specimens of the different groups is clearer. *D. iulia*CLA did not overlap with any other taxon, while some individuals of *D. iulia*CONT and *D. iulia*NLA overlapped with *D. iulia*GA.

In both males and females, the spot pattern elements contributing to variability in PC1 are the absence or presence of the complete bands. PC2 in males reflects the absence or presence of incomplete bands along margins, the transverse band, and a spot at the apex. Variability in females PC2 is similar but also includes the presence or absence of sparse dark scaling around the base of wing.

We noted a high variability in the amount of black scaling on the FW in males of the continental subspecies *D. iulia moderata*, included within *D. iulia*CONT in the analyses. Half of the 42 *moderata* male specimens have a pattern reduced to various degrees, with some specimens having only thin black FW margins. The rest of the males and all 62 *alcionea* males, the other continental subspecies, have the black pattern of FW complete as described above.

Colour pattern of Dryas *mature larvae*

The examination of the colour pattern of the fifth instar larvae of *Dryas* supports the four groups. Main differences are related to the colour pattern of the head capsule and the extension of the white pinacula on the body (Fig. 8). These characters were constant in the larvae we reared and in the reviewed literature and images. The head capsule is orange with frontal black spots in all groups (Fig. 8a–f), except *D. iulia*CONT where the frons is white with black spots and there are twin red spots on the occiput (Fig. 8g,h). White pinacula are well developed, at least laterally, on the body of all taxa except in *D. iulia*GA (Fig. 8g,h). In *D. iulia*CONT, the white pinacula gradually disappear toward the dorsum, whereas they are enlarged and encircle the abdominal segments A2, A4 and A6 in *D. iulia*CLA. In *D. iulia*NLA, there are distinctive white pinacula covering the dorsum of these segments but they are separated from the lateral pinacula, all are quite contrasting over the predominantly black integument (Fig. 8d). In *D. iulia*GA, the integument is variable in colour and the white pinacula are usually reduced, and individuals lack dorsal white pinacula bearing the dorsal scoli on segments A2, A4 and A6 in *D. iulia*NLA (Fig. 8a–c). We also noted that prolegs and areas
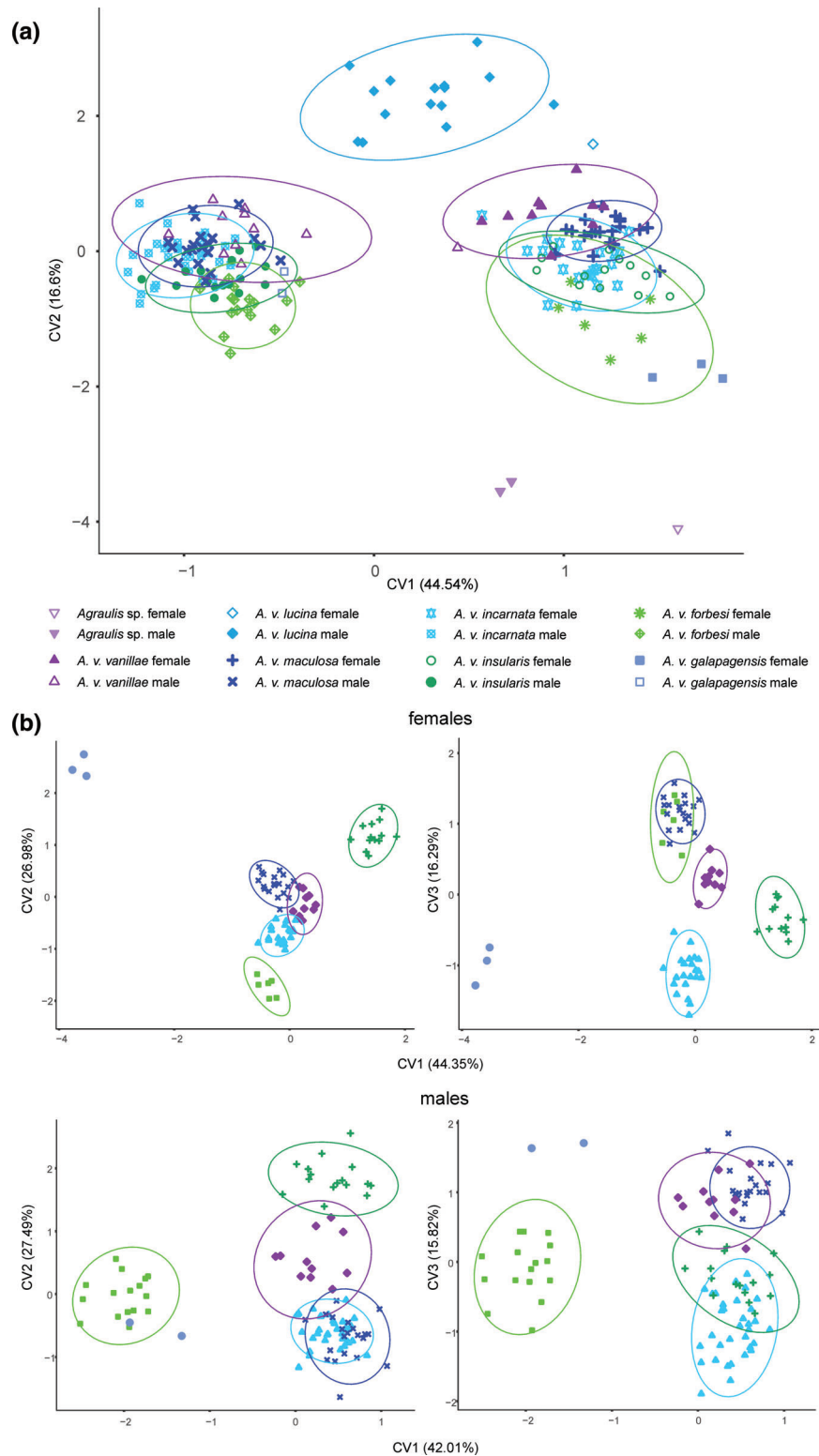
Fig. 5. Discriminant analysis of *Agraulis* taxa using the landmark data of both wings combined after the Procrustes superimposition of each wing separated. (a) All taxa. (b) Males and females separated after the removal of the two most divergent taxa, *Agraulis* sp. and *A. v. lucina*. Equal-frequency ellipses contain approximately 95% of the data points. No ellipses drawn for groups with three or less specimens.
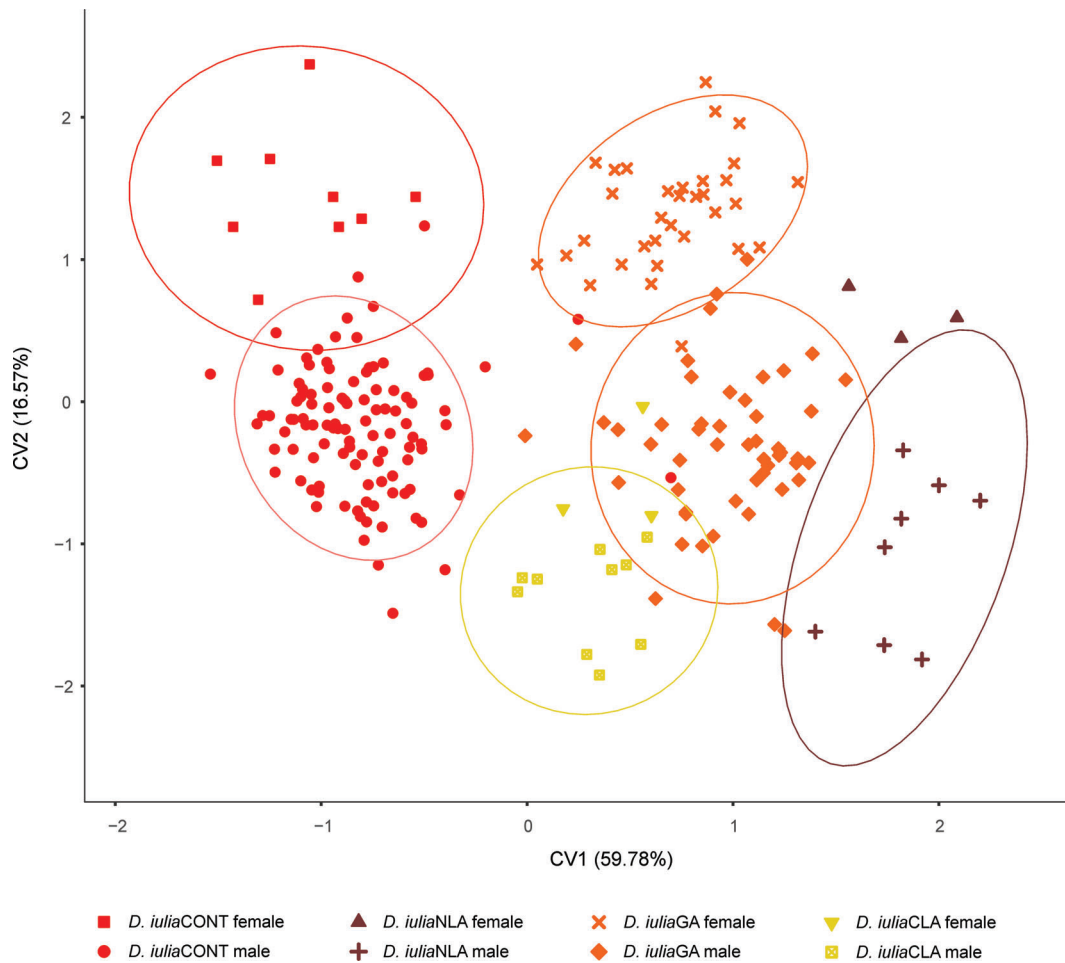
Fig. 6. Discriminant analysis of all *Dryas* taxa. Landmark data of both wings combined after the Procrustes superimposition of each wing separated. Equal-frequency ellipses contain approximately 95% of the data points. No ellipses drawn for groups with three or less specimens.

between the lateral white pinacula are maroon in *D. iulia*CONT and *D. iulia*CLA (Fig. 8e–h), whereas they are orange, brown or black in *D. iulia*GA and *D. iulia*NLA (Fig. 8a–d).

Geographic distribution of Agraulis and Dryas

Both genera are distributed throughout the Neotropics, including the West Indies, although their range also extends northwards outside the tropics, with *Agraulis* reaching the northern upper third of the United States during summer (Figs 9, 10).

In *Agraulis*, the distribution of most taxa includes contact zones or very closely abutting ranges (Fig. 9). All named South American taxa and *Agraulis* sp. are in contact or in very close proximity with at least one congener. Central American *incarnata* reaches northwestern Colombia, where *vanillae* occurs being also found northwards to Panama (Fig. 9). We sequenced one *A. v. vanillae* specimen from northern Ecuador. Both subspecies inhabiting the United States meet in the southern central states. The distributional limits of *Agraulis* taxa living on the Antilles are distinct but again they are in close proximity

to each other. Subspecies *vanillae* and *insularis* are separated by the 40 km of sea between Dominica and Martinique, at the limits of their respective ranges. There are several *A. v. insularis* specimens at the MCZ collected at the Bonacca Islands, just 30 km from Honduras, where *incarnata*, the taxon inhabiting most of Central America, is expected to be present. These *insularis* specimens were collected more than 500 km away from the nearest island harbouring other known *insularis* populations (Fig. 9).

Regarding *Dryas*, its subspecies and the four species appear to have an allopatric distribution. However, there is a contact zone between subspecies *alcionea* and *moderata* in northwestern South America (Fig. 10).

Taxonomic treatment and identification keys

The species from our multilocus species delimitation analyses are supported by the COI barcode comparisons, either by the distance and character approaches, or at least one of them. For *Dryas*, the re-examination of Davies & Bermingham's (2002)
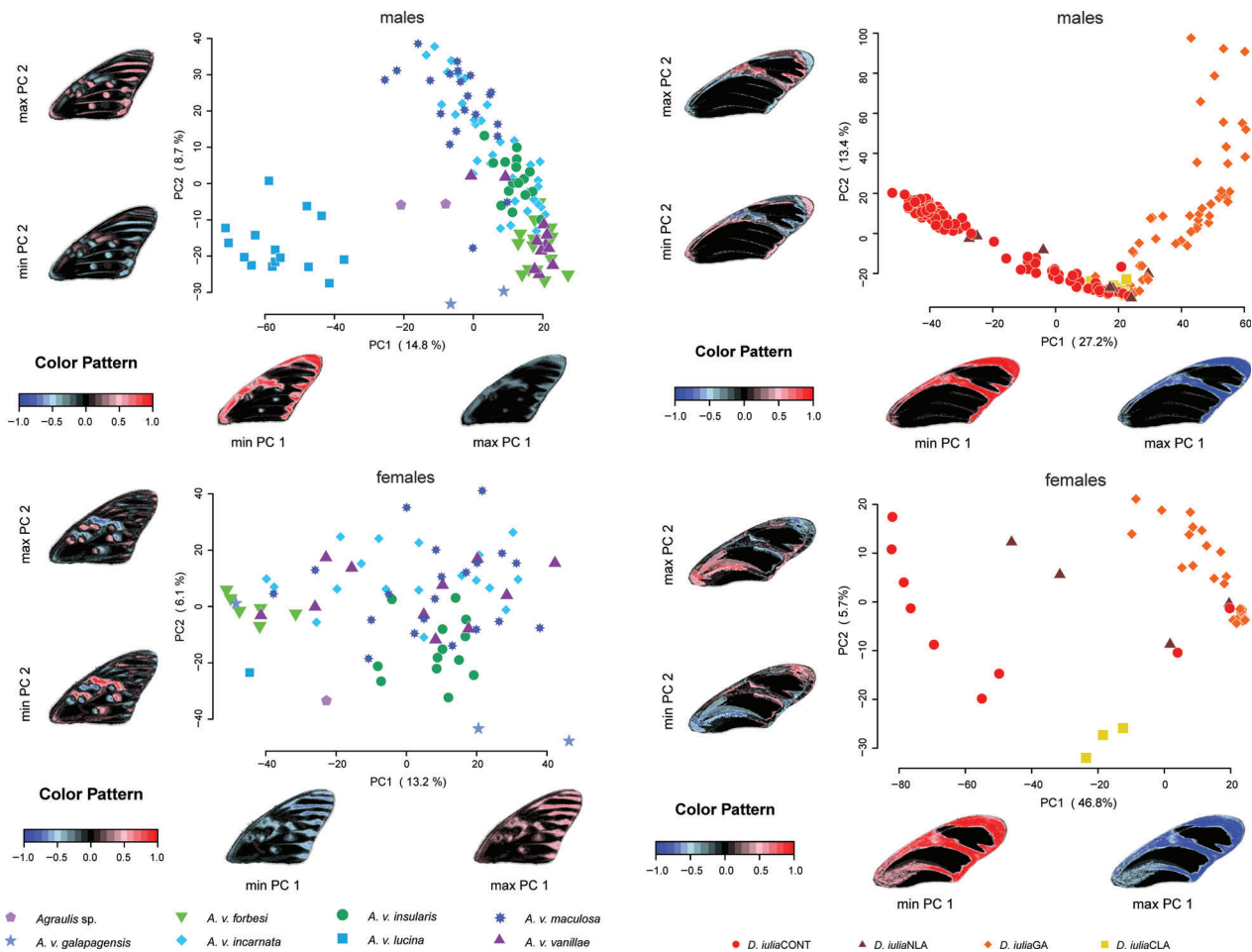
Fig. 7. Principal Component Analysis of the black spot pattern variation on the forewing of each sex of *Agraulis*, left and *Dryas* performed in patternize. Images at the extreme of each principal component show the change at each axis. The mean spot pattern for each species hypothesis is shown in Figure S15.

allozyme frequencies yielded the same four species hypotheses. All these entities can be distinguished by their wing shape and many of them also by their wing length, aspect ratio and FW spot pattern. The available data on *Dryas* mature larvae support the same groupings. The molecular and morphological variability in both genera across their Neotropical range, with distributional limits not always explained by geographic barriers, points to a specific rather than subspecific status for these entities, leading us to propose a new taxonomic treatment. This new treatment addresses only the species-level classification, since a more detailed assessment is needed at the subspecies level, mainly in *Dryas* where several subspecific taxa remain. Regarding *Agraulis*, due to the long debate concerning its possible synonymy with *Dione*, we performed a comparative analysis of all the data sources available to us (Appendix S3) that led us to conclude they are best kept as separate genera. Identification keys are based only on adult external morphology. We used only features if present in more than 85% of the specimens examined. Separate keys are provided for male and female *Dryas* due to their dimorphism.

Agraulis Boisduval and Le Conte, [1835]
Agraulis incarnata (Riley)
  Agraulis incarnata incarnata (Riley)
    Dione vanillae incarnata Riley, 1926: 243
  Agraulis incarnata nigrior Michener
    Agraulis vanillae nigrior Michener, 1942: 7
Agraulis vanillae (Linnaeus)
  Papilio vanillae Linnaeus, 1758: 482
Agraulis forbesi Michener, **new status**
  Agraulis vanillae forbesi Michener, 1942: 3
Agraulis insularis Maynard, **reinstated status**
  Agraulis insularis Maynard, 1889: 89
Agraulis maculosa (Stichel), **new status**
  Dione vanillae maculosa Stichel, [1908]: 18
Agraulis lucina C. Felder & R. Felder, **reinstated status**
  Agraulis lucina C. Felder & R. Felder, 1862: 110
Agraulis galapagensis Holland, **new status**
  Agraulis vanillae var. *galapagensis* Holland, 1890: 194
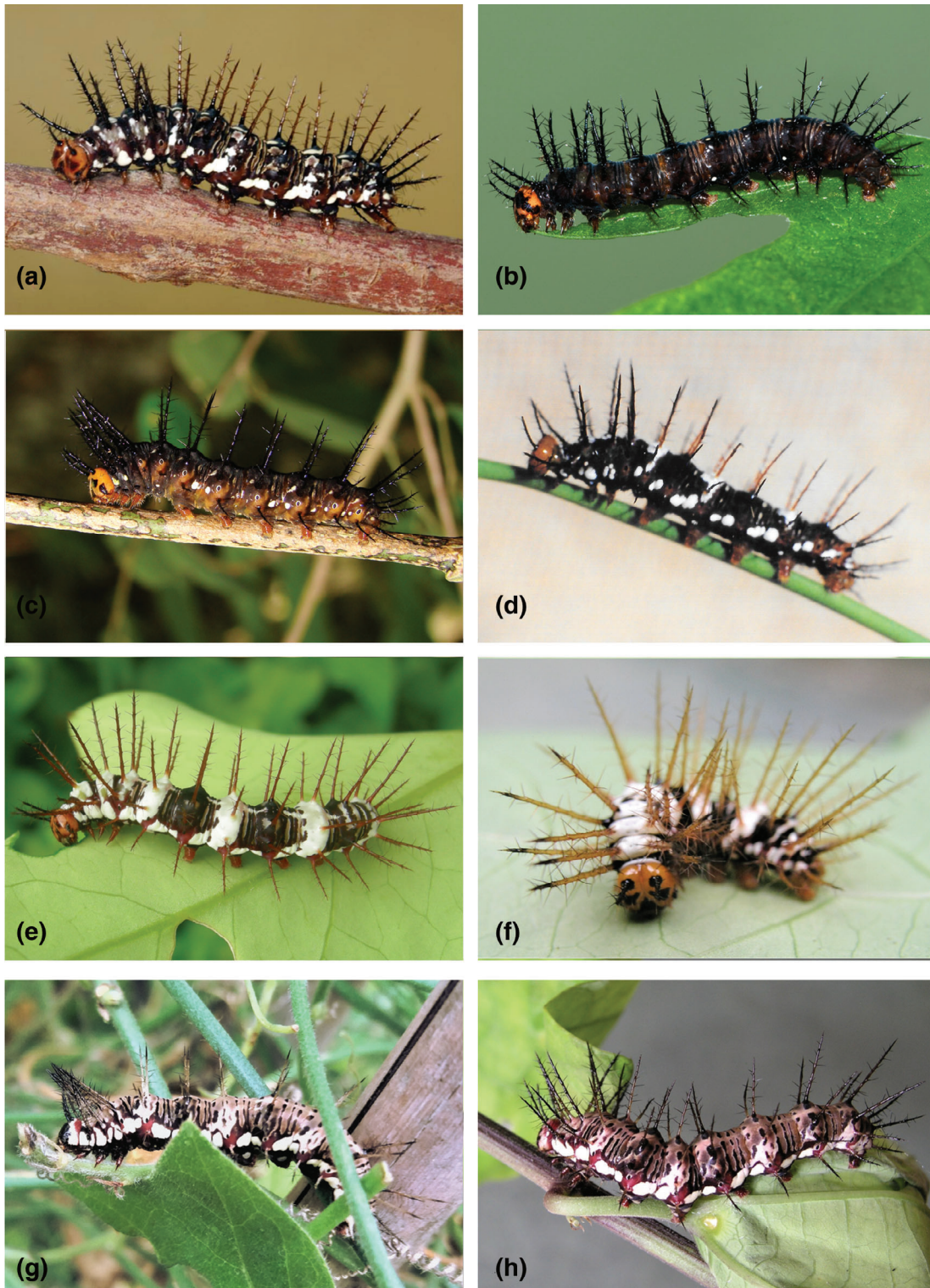*Agraulis* sp. (undescribed species)

Fig. 8. Habitus of the mature larvae of each *Dryas* species hypothesis. *D. iulia*GA: (a, b) *D. iulia iulia*, (a) Puerto Rico, (b) *D. iulia fucatus*, Dominican Republic. (c) *D. iulia carteri*, Cuba. *D. iulia*NLA, (d) *D. iulia dominicana*, Guadeloupe. *D. iulia*CLA, (e, f) *D. iulia martinica*, Martinique. *D. iulia*CONT, (g) *D. iulia moderata*, Costa Rica. (h) *D. iulia alcionea*, French Guiana. Copyright: Alfredo Colon, Carlos de Soto Molinari, R. Núñez and C. Brevignon.
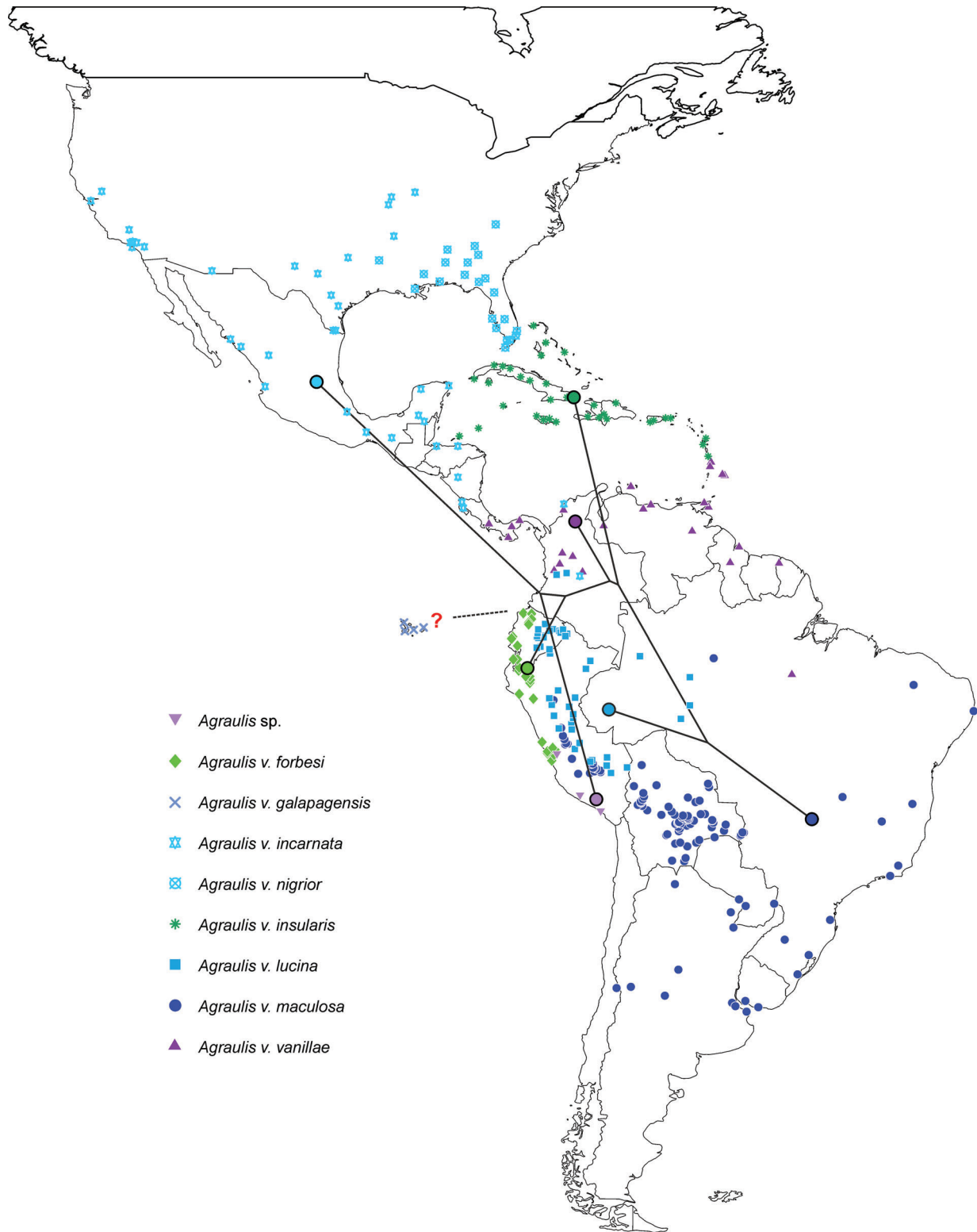
Fig. 9. Relationships and geographic distribution of *Agraulis* taxa based on the data of specimens reviewed by the authors. Colours represent species hypotheses. Question mark indicating the unknown relationships of *A. v. galapagensis*.
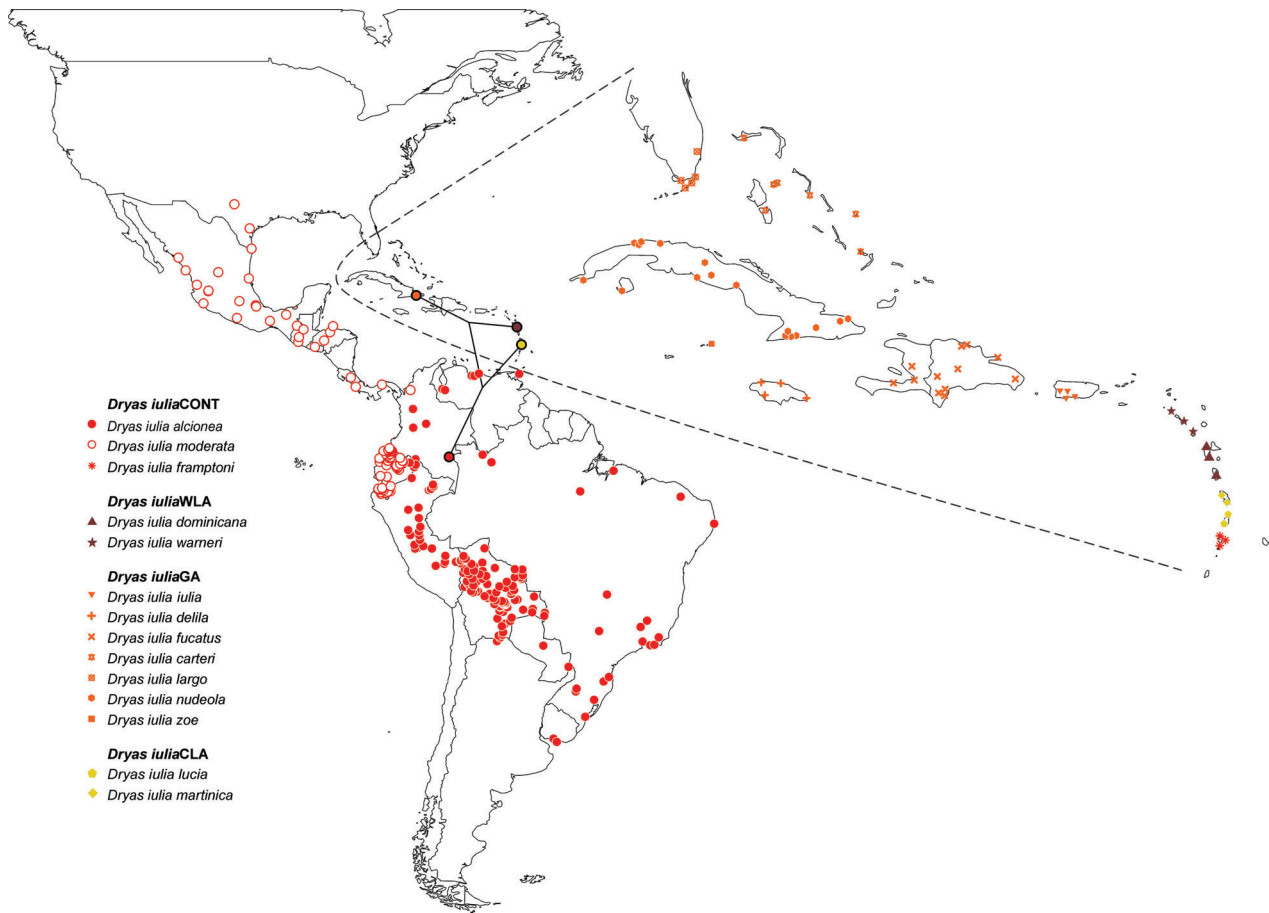
Fig. 10. Relationships and geographic distribution of *Dryas* taxa based on the data of specimens reviewed by the authors. Colours represent species hypotheses.

Key to *Agraulis* species

1. HW 0.6 or less the length of FW (Fig. 5); most upper side of forewing (UPFW) black spot spots connected forming bands; silver spots almost absent from UNHW; western half of the Amazonian region . . . . *A. lucina*
  - HW 0.62 or more the length of FW (Fig. 5); UPFW spots isolated not forming bands; silver spots covering all UNHW; other range 2
2. Smaller species, FWL 27 mm or less; all black spots on UP of wings enlarged 3
  - Larger species, FWL 29 mm or more; at least some black spots on UP of wings reduced 4
3. HW 0.69 or more the length of FW (Fig. 5); an extra black spot on UPHW Cu1-Cu2 cell; dry areas of Peru and northern Chile, west of the Andes . . . . *Agraulis* sp.
  - HW 0.68 or less the length of FW (Fig. 5); no extra black spot on UPHW Cu1-Cu2 cell; Galapagos Islands . . . .
    . . . . *A. galapagensis*
4. Mean FWL 37 mm, range 39–34 mm (Fig. 5); usually 3 silvery pupils on UPFW cell black spots; south U.S.A. to

Panama, but probably also on north Colombia . . . .
. . . . *A. incarnata*
  - Mean FWL smaller than 35 mm, range 36–29 mm (Fig. 5); 2 or 1 silvery pupils on UPFW cell black spots; Panama to central South America and the West Indies . . .
   5
5. UPFW post discal black spot usually separated from spot at cell apex 6
  - UPFW post discal black spot usually close to spot at cell apex 7
6. HW 0.61–0.63 the length of FW (Fig. 5); dry areas of northern Peru and Ecuador, west of the Andes . . . .
    . . . . *A. forbesi*
  - HW 0.66–0.68 the length of FW (Fig. 5); central South America south to the Amazonian region and to the east of the Andes . . . . *A. maculosa*
7. Mean FWL 31 mm, range 33–29 mm (Fig. 5); UPFW post discal black spot at M3-Cu1 and Cu1-Cu2 usually well developed, West Indies north of Martinique . . . .
    . . . . *A. insularis*
  - Mean FWL 34 mm, range 36–31 mm (Fig. 5); at least one of the post discal black spots at UPFW M3-Cu1 and

Cu1-Cu2 usually reduced or absent; West Indies south of Dominica, Panama and northern South America . . . . *A. vanillae*

Dryas Hübner, [1807]
Dryas iulia (Fabricius), treated in previous pages as *D. iulia*GA
    Dryas iulia iulia (Fabricius)
        Papilio iulia Fabricius, 1775: 509
    Dryas iulia fucatus (Boddaert)
        Papilio fucatus Boddaert, 1783: 5
    Dryas iulia carteri (Riley)
        Colaenis iulia carteri Riley, 1926: 240
    Dryas iulia nudeola (Bates)
        Colaenis iulia nudeola Bates, 1934: 168
    Dryas iulia largo Clench
        Dryas iulia largo Clench, 1975: 230
    Dryas iulia zoe Miller & Steinhauser
        Dryas iulia zoe Miller & Steinhauser, 1992: 120
Dryas dominicana (Hall), **revised status**, treated in previous pages as *D. iulia*NLA
    Dryas dominicana dominicana (Hall)
        Colaenis iulia var. *dominicana* Hall, 1917: 161
    Dryas dominicana warneri (Hall), **revised status**
        Colaenis iulia warneri Hall, 1936: 276
Dryas lucia (Riley), **revised status**, treated in previous pages as *D. iulia*CLA
    Dryas lucia lucia (Riley)
        Colaenis iulia lucia Riley, 1926: 241
    Dryas lucia martinica Enrico & Pinchon, **revised status**
        Dryas iulia martinica Enrico & Pinchon, 1969: 82
Dryas alcionea (Cramer), **reinstated status**, treated in previous pages as *D. iulia*CONT
    Dryas alcionea alcionea (Cramer)
        Papilio alcionea Cramer, 1779: 38
    Dryas alcionea moderata (Riley), **revised status**
        Colaenis iulia moderata Riley, 1926: 241
    Dryas alcionea framptoni (Riley), **revised status**
        Colaenis iulia framptoni Riley, 1926: 241

Key to *Dryas* species

1. Veins of outer half UPFW covered with black androconial scale, males 2
- Veins of outer half UPFW not covered with black androconial scales, females 5
2. Small species, mean FWL 38 mm, range 36–39 mm (Fig. 5); UP of wings bright reddish orange with sparse black scaling along outer margins and black spots on apex and on mid costa (Figure S10); central Lesser Antilles (Martinique, St. Lucia) . . . . *D. lucia*
- Larger species, mean FWL 41 mm, range 38–43 mm (Fig. 5); UP of wings bright reddish orange, orange or pale orange, black scaling pattern variable (Figure S10); other Antillean islands and the continent 3

3. UP of wings bright reddish orange with solid black bands along outer margins, FW costa, and transversal on FW (Figure S10)[*]; continent and southern Lesser Antilles (St. Vicent, Grenadines, Grenada) . . . . *D. alcionea*
- UP of wings pale orange with faint black bands along outer margins; transversal black band of FW absent, incomplete, or present but never solid; northern Lesser Antilles and Greater Antilles 4
4. UPFW with two faint black bands: a complete transversal and a short subapical, apex orange (Figure S10); northern Lesser Antilles (St. Kitts, Monserrat, Saba, Guadeloupe, Dominica) . . . . *D. dominicana*
- UPFW with black scaling reduced to spots or an incomplete fainter transverse band (Figure S10); Greater Antilles, Bahamas and south Florida … … … … *D. iulia*
5. UP wings pale orange brown, black bands faint and incomplete (Figure S10); Greater Antilles, Bahamas and south Florida . . . .*D. iulia*
- UP of wings orange or reddish orange, black bands faint and incomplete or solid and complete (Figure S10); other range 6
6. UP of wings orange sparsely covered with black scaling, black bands solid (Figure S10); continent and southern Lesser Antilles (St. Vicent, Grenadines, Grenada) . . . . *D. alcionea*
- UP of wings pale orange or reddish orange not distinctly covered with sparse black scaling, black bands faint (Figure S10); central and northern Lesser Antilles 7
7. UP of wings pale orange, black band only on the distal third of 1A at FW (Figure S10); northern Lesser Antilles . . . . *D. dominicana*
- UP of wings reddish orange, no black band on 1A at FW (Figure S10); central Lesser Antilles . . . . *D. lucia*

[*]21 of the 142 males of *D. alcionea* lacked black scaling on the FW).

Discussion

The results of our coalescent-based species delimitation analyses and model testing rejected *Agraulis* and *Dryas* as monotypic. All our species hypotheses received the strongest support and were recovered as monophyletic in the coalescent phylogenetic reconstructions. Although molecular species delimitation methods have been regarded only as detectors of genetic structure (Sukumaran & Knowles, 2017), the other data sources available to us support these species hypotheses.

COI barcodes, while adding a wider geographic coverage, also serve to diagnose all species, despite the low genetic distances between some sister taxa. Whereas values around 2% are often used as a threshold between intra and interspecific distances in Lepidoptera (Hebert *et al.*, 2010; Mutanen *et al.*, 2012), there are examples of species pairs differing by around 1% or even less, as found by Hebert *et al.* (2004), Burns *et al.* (2007), Hausmann *et al.* (2011) and Cong *et al.* (2016), among others. The character-based approach allowed diagnosis

of all species in both genera. Even when some of these taxa lack individual diagnostic positions, for example, *A. maculosa* and *D. iulia*, the unique combination of characters shared only with some of the other taxa allowed their recognition. Character-based approaches have been successful in identifying species when distance and reciprocal monophyly methods have failed (Zou *et al.*, 2011; Wang *et al.*, 2019). In our COI dataset, paraphyly only affects *D. lucia*, which appears nested within *D. alcionea*. However, these two species are separated by a mean distance of 1.86%. Distances from *D. lucia* to the other two *Dryas* species are above 3%. The genetic distances among our barcode sequences are similar to those calculated by Davies & Bermingham (2002), who used COI/II and a larger sample of individuals.

Agraulis lineages to the west of the Andes and in Central & North America (*A. incaranata*, *A. forbesi* and *Agraulis* sp.) seem to be old, ca. 8.59–2.8 Ma according to our estimations (Figure S3). However, the *Agraulis* species to the east of the Andes and both species pairs within *Dryas* originated after an initial split and are recent (1.38–1.41 Ma, Figure S3). The low levels of interspecific divergence between some pairs of taxa are consistent with recent speciation, for example, the *Agraulis* clade inhabiting east of the Andes and the Antilles, and in the *D. iulia-D. dominicana* pair. Another possible explanation is introgression, which may have occurred, for example, between pairs of taxa such as *A. maculosa* and *A. lucina*, which according to our results are of very recent origin (0.69 Ma) and that have a large contact zone. Indeed, we have examined specimens that seem to represent hybrids among these two species: FW shorter and broader as in *A. maculosa* with heavier marks on the upperside and almost no trace of silver spots at the underside as in *A. lucina*. Specimens with that mix of characters have been reported in the literature from localities at the contact zone of *A. maculosa* and *A. lucina*, and have been even named (Stichel, 1908; Brown & Mielke, 1972). However, there are no studies to date focused on what proportion of these hybrids exist within natural populations, if hybrids occur all along the contact zone or only at specific localities, and the effect of interbreeding on their genomes. We acknowledge our limited sampling and the small number of genes sequenced, but since our sequences show consistent differences between *A. maculosa* and *A. lucina*, and given the marked differences in their wing shape and pattern, we prefer to treat them as species rather than subspecies. Recently Zhang *et al.* (2020) also proposed a split within *Agraulis* after comparing COI barcode and nuclear genome data from *A. insularis* and *A. incarnata* populations.

The re-examination of Davies & Bermingham's (2002) allozyme data also supports the existence of four distinct groups within *Dryas*. Those authors also compared the restriction enzymes Msp-1 and Taq-1 between *D. dominicana*, *D. iulia* and *D. lucia* and found different haplotypes in frequencies above 94 and 83%, respectively.

Ours is the first geometric morphometrics analyses applied to the taxonomy of the genera *Agraulis* and *Dryas*. Past studies have emphasized only the description of phenotypic characters and measurement ranges of FWL and width (Michener, 1942; Emsley, 1963; Clench, 1975). Although limited in resolution,

linear measurements proved to be useful in recognizing several taxa by their size and wing aspect ratio. Geometric morphometrics is a powerful tool that has been increasingly employed in evolutionary studies (Klingenberg, 2010) and to a lesser extent in taxonomy (Schlick-Steiner, 2010; Tatsuta *et al.*, 2018). In our study groups, geometric morphometrics successfully classified most specimens of each species and revealed how wing shape has evolved in the different species, and between the sexes within species. In *Agraulis*, the differences in the position of the cell end and the origin of cubital veins and the elongation or broadening of the FW, among other features, would have remained undetected by the traditional descriptive approach previously used. In *Dryas* taxa, the changes in the shape of the end of cell and the outline of the FW and HW outer margins are worth mentioning. Further work should investigate which selective forces have led to these wing vein/shape configurations. Studies have shown that such differences lead to functional differentiation and that habitat, predation and sex-specific behaviour likely act as major selective forces (Chazot *et al.*, 2016; Le Roy *et al.*, 2019; Penz & Williams, 2020). *Agraulis* and *Dryas* populations face a broad array of ecological conditions across their distributions from the arid Pacific coast to the Amazon basin and the West Indies, which likely have influenced speciation processes, including the wing shape evolution.

Quantification of the FW spot pattern revealed differences in both genera where taxa were previously recognized only by qualitative differences in the 'size' of the spots and their absence or presence (Riley, 1926; Michener, 1942; Clench, 1975). The visualization of the spot pattern and its analysis allowed a more objective comparison among the taxa and the recognition of many of them. With the recent development of several software packages the quantification of colour pattern has contributed to the study of several groups, including flowering plants, butterflies, spiders, fishes and mammals in a more integrative way (Van Belleghem *et al.*, 2017; Morris *et al.*, 2019; Salis *et al.*, 2019; Ortiz-Acevedo *et al.*, 2020).

The mature larvae of each *Dryas* species can be also recognized by the size and colour of their pinacula. The *Dryas* specimens reared by us match the descriptions and illustrations for each taxon in the literature reviewed and in images with locality data available online (Beebe *et al.*, 1960; Rickard, 1968; Paim *et al.*, 2004; Askew & Stafford, 2008; Janzen & Hallwachs, 2009; David & Lucas, 2017; Turner & Turland, 2017; Warren *et al.*, 2017).

Distributional data were important when interpreting the outcome of the molecular, morphometric and FW spot pattern analyses. Our maps matched a previous study that mapped thousands of records within each Heliconiini genus (Rosser *et al.*, 2012), with record sources overlapping only partially. The populations of most *Agraulis* taxa have contact zones or are in close proximity with other congeners, as literature records also illustrate: *A. incarnata nigrior* and *A. insularis* in Cuba, *A. i. incarnata* and *A. vanillae* from Costa Rica to Colombia, *A. forbesi* and *Agraulis* sp. and among *A. lucina*, *A. maculosa* and *A. vanillae* in Brazil, Colombia and Peru (Michener, 1942; de la Torre, 1949a; 1949b; Brown Jr. & Mielke, 1972; Rosser *et al.*, 2012). In the material we examined there are records of *A. vanillae* from

Ecuador, *A. incarnata* from Colombia and *A. insularis* from islands near Honduras and even when some of them could be mislabelled that seems to not to be the case for recently collected *vanillae* specimens by KRW in Ecuador or the *insularis* series at the MCZ. Apparently, the Andean cordillera is a significant barrier between eastern and western species, but there may also be some ecological adaptations that maintain allopatry. For example, *A. forbesi* also occurs in a restricted region east of the Andes, in the headwaters of the Río Marañón, without any prominent geographic barrier separating it from Amazonian *A. lucina*. However, the dry forests of this region also contain a number of butterfly species otherwise endemic to the dry forests of southwestern Ecuador and northwestern Peru. By contrast, sea barriers seem to be permeable to *Agraulis*, *A. insularis* flies from the Bahamas to the northern Lesser Antilles, whereas *A. vanillae* inhabits the islands southward. These islands are separated by 30–100 km wide sea passages. So the 40 km of sea between the ranges of these two taxa in the Lesser Antilles, inhabiting Dominica and Martinique, respectively, unlikely constitute an effective barrier to dispersal. Habitat diversity, island area and their distance to the most likely source of colonists, the continent, do not differ much among these and their neighbouring islands (Ricklefs & Lovette, 1999; Ricklefs & Bermingham, 2007). Hypotheses explaining speciation and the present day distribution of *Agraulis* species require further research, but likely include adaptation to the different habitat types, colonization of new areas followed by periods of isolation and posterior range expansion. The three *Dryas* species in the Antilles apparently descended from two independent colonization events: one more recent giving origin to *D. lucia* and an earlier one by the ancestor of the taxon that subsequently diverged into *D. iulia* and *D. dominicana*. We retained the taxon *framptoni* from the southern Lesser Antilles as a *D. alcionea* subspecies, despite its small size and broader wings, due to the close relationship of these two taxa as indicated by the mitochondrial and allozyme data reported by Davies & Bermingham (2002).

Without performing a formal biogeographic analysis, the evidence is consistent with a west of the Andes origin for *Agraulis*. Two of the earliest diverging lineages, *Agraulis* sp. and *A. forbesi*, occur there. The ancestor of a third old lineage, *A. incarnata*, may have colonized Central and North America through the Panama isthmus, as a land corridor or as chain of islands, though the dates of the emergence/closure of this isthmus remain contentious (Bacon *et al.*, 2015; O'Dea *et al.*, 2016). The aforementioned three taxa exhibit the greatest genetic differentiation within the genus. Despite lacking molecular data for *A. galapagensis*, its isolation and likely origin from an ancestor related to the older west Andes lineages together with its morphological differentiation lead us to propose its specific status. The ancestor of the clade containing the youngest *Agraulis* taxa may have expanded its range by dispersal through northwestern South America to the rest of the continent and the Antilles. A vicariant origin of the taxa to the east of the Andes seems unlikely since the uplift of the mountain chain took place earlier than our inferred date of divergence (Mora *et al.*, 2010). The continental *Agraulis* species may have evolved under different environmental conditions across Central America, the

Chocó region west of the Andes, the Amazon region and the Guianas and the southeastern Atlantic region. These regions seem to have played an important role in the diversification of many South American groups, including butterflies (Smith *et al.*, 2014; Toussaint *et al.*, 2019; Ortiz-Acevedo *et al.*, 2020; Matos-Maraví *et al.*, 2021). However, *Dryas alcionea* (as *D. iulia*CONT in figure 19), which overlaps its range with most continental *Agraulis*, apparently has maintained gene flow among its populations. The available barcodes include shared haplotypes from Yucatán to northern Argentina, subspecies *moderata* and *alcionea*, respectively, and suggest an ongoing gene flow across the range of *D. alcionea moderata*, between Central America and the Pacific coast of South America (Fig. 3). We found no haplotypes shared between *Dryas* populations on both sides of the Andes.

Further efforts should gather more molecular data from a broader sample of individuals, and add information on the immature stages and the ecology of each species, since studies to date have focused on both genera only as single species. Future research could also investigate in depth which factors have affected the evolution of wing shape and colour pattern. Perhaps the most obvious example is *A. lucina* which possesses a highly distinct wing shape and divergent pattern on both wings surfaces in comparison with the remaining species. How this species, apparently of very recent origin, gained these features remains an interesting question together with its occasional apparent hybridization with *A. maculosa* and perhaps also with *A. vanillae*. The gene flow among these and possibly other *Agraulis* species, given their numerous contact zones, is another important research topic. The existence of pre- and postzygotic barriers, the characteristics of these hybrids (*e.g.* complete or incomplete sterility) and the role of mimicry, are all aspects that remain unexplored for these taxa. Further studies could emulate recent research focused on the evolution of the most diverse clade within the Heliconiini, the genus *Heliconius* that have shed light on some of these aspects (Morris *et al.*, 2019; González-Rojas *et al.*, 2020; Massardo *et al.*, 2020; Mérot *et al.*, 2020).

Supporting Information

Additional supporting information may be found online in the Supporting Information section at the end of the article.

Appendix S1. DAT file, PAST format, containing the landmark coordinates of both wings of the *Agraulis* specimens studied. Procrustes transformation was applied to each wing separately.

Appendix S2. DAT file, PAST format, containing the landmark coordinates of both wings of the *Dryas* specimens studied. Procrustes transformation was applied to each wing separately.

Appendix S3. On the generic status of *Agraulis*.

Figure S1. Multilocus coalescent species tree of the *Agraulis* available specimens obtained with StarBeast.

Figure S2. Multilocus coalescent species tree of the *Dryas* available specimens obtained with StarBeast.

Figure S3. STARBEAST2 time calibrated tree for crown age estimation of *Agraulis* and *Dryas*.

Figure S4. Placement of the landmarks employed in the geometric morphometric analyses and linear measurements of *Agraulis* and *Dryas* specimens.Unlabelled landmarks in *Agraulis* are homologous of the landmarks labelled in *Dryas*. Unlabelled landmarks in *Dryas* hindwing represent the mid points between landmarks at the end of veins. Landmarks 1 and 9 and 1 and 14 were used to measure the forewing and hindwing length, respectively.

Figure S5. Species trees of *Agraulis* obtained in BEAST using the nuclear (wingless, TH, Ef1a, apterous), A, and mitochondrial (16S and COI), B, datasets.

Figure S6. Species trees of *Dryas* obtained in BEAST using the nuclear (wingless, TH, Ef1a, apterous), A, and mitochondrial (16S and COI), B, datasets.

Figure S7. Hierarchical clustering of 17 allozymes allelic frequencies from *Dryas* specimens captured from Davies & Bermingham (2002) Appendix II. The tree was obtained with the Ward's method using the Euclidean similarity index and 1000 bootstrap replicates (The UPGMA algorithm with the Bray-Curtis index yielded a similar result not shown in the figure). Colors represent the species hypotheses.

Figure S8. Forewing length – FWL (left), hindwing length – HWL (center) and wings aspect ratio by sex HWL–FWL (right) of *Agraulis* and *Dryas* species hypotheses. See Tables S6 and S7 for the results of the statistical tests. Results of the aspect ratio comparison between indicated by ns – not significant or */ *** – significant/extremely significant.

Figure S9. Scree plots of the landmarks Principal Component Analyses for the forewing and hindwing of *Agraulis* and *Dryas* specimens.

Figure S10. Thin-plate splines deformation grids representing shape change from the female to the male mean form, all specimens, in *Agraulis* and *Dryas*. The extremes of the colour scales represent shape expansion, higher values, or compression, lower values.

Figure S11a. Thin-plate spline deformation grids showing the shape change in the wings of each *Agraulis* taxon. (a) From the mean shape of females to the mean shape of males. The extremes of the colour scales represent shape expansion, higher values, or compression, lower values.

Figure S11b. Thin-plate spline deformation grids showing the shape change in the wings of each *Agraulis* taxon. (b) Males, from the mean form (all specimens) to the mean form

of each taxon. The extremes of the color scales represent shape expansion, higher values, or compression, lower values (cont.).

Figure S11c. Thin-plate spline deformation grids showing the shape change in the wings of each *Agraulis* taxon. (c) Females, from the mean form (all specimens) to the mean form of each taxon (cont.).

Figure S12. Thin-plate splines deformation grids representing examples of wings shape change between the mean forms of *Agraulis* and *Dryas* taxa pairs. The extremes of the colour scales represent shape expansion, higher values, or compression, lower values.

Figure S13a. Thin-plate spline deformation grids showing the shape change in the wings of each *Dryas* taxon. (a) From the mean shape of females to the mean shape of males. The extremes of the colour scales represent shape expansion, higher values, or compression, lower values.

Figure S13b. Thin-plate spline deformation grids showing the shape change in the wings of each *Dryas* taxon. (b) From the mean shape of the genus (all specimens) to the mean shape of each sex within each taxon. The extremes of the color scales represent shape expansion, higher values, or compression, lower values.

Figure S14. Percentage of shape change, on both wings and on each wing separated, on each *Agraulis* and *Dryas* species hypothesis by sex with the genus mean form, all specimens, as reference and between sexes, from the female mean form to the mean male form. Percentage per landmark shown in Tables S8 and S9. The extremes of the colour scales represent the percentage of change, higher (blue) or lower (blue).

Figure S15. Forewing mean spot pattern for males and females of *Agraulis* and *Dryas* species hypotheses obtained in the ʀ package patternize. No pattern was obtained for females of *Agraulis* sp. and *A. v. lucina* since a single specimen was available in each case. The extremes of the colour scales represent dark scaling expansion, higher values, or no dark scaling, lower values.

Table S1. Vouchers and GenBank accession numbers of the sequences included in the six markers dataset for the divergence times estimations for the crown age of *Agraulis* and *Dryas* and the multilocus species delimitation analyses in BPP. X indicates sequences shorter than 200 bp no accepted in GenBank.

Table S2. List of *Agraulis* and *Dryas* specimens with accession numbers of their COI barcode sequences.

Table S3. Coordinates of *Agraulis* and *Dryas* specimens employed for distribution maps.

Table S4. Species hypotheses of *Agraulis* obtained in each iBPP run with molecular and morphometric datasets combined. Prior parameters, algorithms and their ε (0) or α and m (1) values and posterior probabilities for the resulting species hypotheses are shown for each run.

Table S5. Species hypotheses of *Dryas* obtained in each iBPP run with molecular and morphometric datasets combined. Prior parameters, algorithms and their ε (0) or α and m (1) values and posterior probabilities for the resulting species hypotheses are shown for each run.

Table S6. Character-based DNA barcodes for species hypotheses within the genera *Agraulis* and *Dryas*. Colours represent the four nucleotides types. Numbers of sequences per taxa are given in brackets. Positions with two character states are given only when one of them is present in more than the 90% of the samples.

Table S7. Comparisons through PERMANOVA tests of wings linear measurements among the species hypotheses within *Agraulis*. P-values and F statistics shown in each case. FWL- forewing length, WR- wings aspect ratio, by sex: HWL/FWL. 10 000 permutations ran at each test. Not significant p > 0.05 values shown in bold.

Table S8. Comparisons through PERMANOVA tests of wings linear measurements among the species hypotheses within *Dryas*. p-values and the F statistics shown in each case. FWL- forewing length, HWL hindwing length, WR- wings aspect ratio, by sex: HWL/FWL. 10 000 permutations ran at each test. Not significant p > 0.05 values shown in bold.

Table S9. Eigenvalues, percent of variance explained and variables, landmarks, contribution to the Principal Component Analyses of the forewing and hindwing of *Agraulis* specimens. In bold meaningful PCs, according to scree plots (Figure S4), and variables with the major contribution to the total variability of the data at each PC.

Table S10. Eigenvalues, percent of variance explained and variables, landmarks, contribution to the Principal Component Analyses of the forewing and hindwing of *Dryas* specimens. In bold meaningful PCs, according to scree plots (Figure S4), and variables with the major contribution to the total variability of the data at each PC.

Table S11. Procrustes distances /p-values after 10 000 permutations among fore (FW) and hindwing (HW) shape configurations of the *Agraulis* species hypotheses. Lower left matrices males, upper right females. In bold p values above 0.05 indicating not significant differences.

Table S12. Procrustes distances /p-values after 10 000 permutations among fore (FW) and hindwing (HW) shape configurations of the *Dryas* species hypotheses. Lower left

matrices males, upper right females. In bold p values above 0.05 indicating not significant differences.

Table S13. Percent of shape change at landmarks on the forewing of males and females on each *Agraulis* and *Dryas* species hypothesis with respect to the mean shape of each genus and from the female mean shape to the male mean shape within each species hypothesis. In bold values above 10% and 100% in the TOTAL column.

Table S14. Percent of shape change at landmarks on the hindwing of males and females on each *Agraulis* and *Dryas* species hypothesis with respect to the mean shape of each genus and from the female mean shape to the male mean shape within each species hypothesis. In bold values above 10% and 100% in the TOTAL column.

Data availability statement

The data that support the findings of this study are available in the supplementary material of this article. All sequences,

including the newly generated are available in GenBank and their accession numbers appear in Tables S1 and S2. Files containing the landmarks data for each genus have been included in the supplementary material.

References

Askew, R.R. & Stafford, P.A.V.B. (2008) *Butterflies of the Cayman Islands*. Apollo Books, Stenstrup.

Bacon, C.D., Silvestro, D., Jaramillo, C., Smith, B.T., Chakrabarty, P. & Antonelli, A. (2015) Biological evidence supports an early and complex emergence of the Isthmus of Panama. *Proceedings of the National Academy of Sciences USA*, **112**, 6110–6115 E3631.

Baele, G., Li, W.L.S., Drummond, A.J., Suchard, M.A. & Lemey, P. (2013) Accurate model selection of relaxed molecular clocks in Bayesian phylogenetics. *Molecular Biology and Evolution*, **30**, 239–243.

Bai, Y., Dong, J.-J., Guan, D.-L., Xie, J.-Y. & Xu, S.-Q. (2016) Geographic variation in wing size and shape of the grasshopper *Trilophidia annulata* (Orthoptera: Oedipodidae): morphological trait variations follow an ecogeographical rule. *Scientific Reports*, **6**, 32680.

Beebe, C.W., Crane, J. & Fleming, H. (1960) A comparison of eggs, larvae and pupae in fourteen species of heliconiine butterflies from Trinidad, W.I. *Zoologica*, **45**, 111–154.

Beltrán, M., Jiggins, C.D., Brower, A.V.Z., Bermingham, E.P. & Mallet, J.L.B. (2007) Do pollen feeding, pupal-mating and larval gregariousness have a single origin in *Heliconius* butterflies? Inferences from multilocus DNA sequence data. *Biological Journal of the Linnean Society*, **92**, 221–239.

Beltrán, M., Jiggins, C.D., Bull, V., Linares, M., Mallet, J.L.B., McMillan, W.O. & Bermingham, E.P. (2002) Phylogenetic discordance at the species boundary: comparative gene genealogies among rapidly radiating *Heliconius* butterflies. *Molecular Biology and Evolution*, **19**, 2176–2190.

Benson, W.W., Brown, K.S. Jr & Gilbert, L.E. (1976) Coevolution of plants and herbivores: passion flower butterflies. *Evolution*, **29**, 659–680.

Bookstein, F.L. (1989) Principal warps: Thin-plate splines and the decomposition of deformations. *IEEE Transactions on Pattern Analysis and Machine Intelligence*, **11**, 567–585.

Bouckaert, R., Heled, J., Kuehnert, D. *et al.* (2014) BEAST 2: a software platform for Bayesian evolutionary analysis. *PLoS Computational Biology*, **10**, e1003537.

Breuker, C.J., Gibbs, M., Van Dongen, S., Merckx, T. & Van Dyck, H. (2010) The use of geometric morphometrics in studying butterfly wings in an evolutionary ecological context. *Morphometrics for Nonmorphometricians* (ed. by A.M.T. Elewa), pp. 271–287. Springer-Verlag, Berlin Heidelberg.

Brower, A.V.Z. & Egan, M.G. (1997) Cladistic analysis of *Heliconius* butterflies and relatives (Nymphalidae: Heliconiiti): a revised phylogenetic position for *Eueides* based on sequences from mtDNA and a molecular gene. *Proceedings of the Royal Society of London (B)*, **264**, 969–977.

Brown, K.S. Jr. (1981) The biology of *Heliconius* and related genera. *Annual Review of Entomology*, **26**, 427–456.

Brown, K.S. Jr & Mielke, O.H.H. (1972) The heliconians of Brazil (Lepidoptera: Nymphalidae). Part II. Introduction and general comments, with a supplementary revision of the tribe. *Zoologica*, **57**, 1–40.

Bull, V., Beltrán, M., Jiggins, C.D., McMillan, W.O., Bermingham, E.P. & Mallet, J.L.B. (2006) Polyphyly and gene flow between non-sibling *Heliconius* species. *BMC Biology*, **4**, 1–17.

Burns, J.M., Janzen, D.H., Hajibabaei, M., Hallwachs, W. & Herbert, P.D.N. (2007) DNA barcodes of closely related (but morphologically and ecologically distinct) species of skipper butterflies (Hesperiidae) can differ by only one to three nucleotides. *Journal of the Lepidopterists' Society*, **61**, 138–153.

Chazot, N., Panara, S., Zilbermann, N. *et al.* (2016) *Morpho* morphometrics: shared ancestry and selection drive the evolution of wing size and shape in *Morpho* butterflies. *Evolution*, **70**, 181–194.

Chazot, N., Wahlberg, N., Freitas, A.V.L. *et al.* (2019) Priors and posteriors in Bayesian timing of divergence analyses: the age of butterflies revisited. *Systematic Biology*, **65**, 797–813.

Clench, H.K. (1975) Systematic notes on *Dryas iulia* (Heliconiidae). *Journal of the Lepidopterists' Society*, **29**, 230–235.

Cong, Q., Shen, J., Warren, A.D., Borek, D., Otwinowski, Z. & Grishin, N.V. (2016) Speciation in Cloudless Sulphurs Gleaned from Complete Genomes. *Genome Biology and Evolution*, **8**, 915–931.

da Silva, D.S., Dell'Erba, R., Kaminski, L.A. & Moreira, G.R.P. (2006) Morfologia externa dos estágios imaturos de heliconíneos neotropicais: V. *Agraulis vanillae maculosa* (Lepidoptera, Nymphalidae, Heliconiinae). *Iheringia, Serie. Zoologica*, **96**, 219–228.

Daniels, J.C. (2009) Gulf Fritillary Butterfly, *Agraulis vanillae* (Linnaeus) (Insecta: Lepidoptera: Nymphalidae). *EENY*, **423**, 1–3.

David, G. & Lucas, P.-D. (2017) *Atlas des papillons de jour de la Martinique*. Fort-de-France: Association Martinique Entomologie. Available at: http://transfaire.antilles.inra.fr/IMG/pdf/ob_dfda24_atlas-des-papillons-de-jour-de-la-mart_copie.compressed.pdf.

Davies, N. & Bermingham, E.P. (2002) The historical biogeography of two Caribbean butterflies (Lepidoptera: Heliconiidae) as infrerred from genetic variation at multiple loci. *Evolution*, **56**, 573–589.

de la Torre, S.L. (1949a) A list supplementing Bates' "Butterflies of Cuba". *Lepidopterists' News*, **3**, 65.

de la Torre, S.L. (1949b) Géneros y especies de la subfamilia Heliconiinae hallados en Cuba (Lepidoptera. Nymphalidae) (Adiciones y correcciones al catálogo de Cuba). *Memorias de la Sociedad Cubana de Historia Natural*, **19**, 191–194.

Dryden, I.L. & Mardia, K.V. (1998) *Statistical Shape Analysis*. John Wiley & Sons, New York, New York.

Dworkin, I. & Gibson, G. (2006) Epidermal growth factor receptor and transforming growth factor beta signaling contributes to variation for wing shape in *Drosophila melanogaster*. *Genetics*, **173**, 1417–1431.

Emsley, M.G. (1963) A morphological study of imagine Heliconiinae (Lep.: Nymphalidae) with a consideration of the evolutionary relationships within the group. *Zoologica*, **48**, 85–130.

González-Rojas, M.F., Darragh, K., Robles, J. *et al.* (2020) Chemical signals act as the main reproductive barrier between sister and mimetic *Heliconius* butterflies. *Proceedings of the Royal Society B*, **287**, 20200587.

Goonesekera, K., van der Poorten, G. & Ranawaka, G.R. (2018) Morphometry as a tool in species identification: a study with special reference to species of the genus *Mycalesis* (Lepidoptera: Nymphalidae). *Journal of National of Sciences Foundation of Sri Lanka*, **46**, 311–328.

Hammer, Ø., Harper, D.A.T. & Ryan, P.D. (2001) PAST: Paleontological statistics software package for education and data analysis. *Palaeontologia Electronica*, **4**, 9.

Hastie, T., Tibshirani, R. & Buja, A. (1994) Flexible discriminant analysis by optimal scoring. *Journal of the American Statistical Association*, **89**, 1255–1270.

Hausmann, A., Haszprunar, G. & Hebert, P.D.N. (2011) DNA Barcoding the Geometrid Fauna of Bavaria (Lepidoptera): Successes, Surprises, and Questions. *PLoS ONE*, **6**, e17134.

Hebert, P.D.N., Penton, E.H., Burns, J.M., Janzen, D.H. & Hallwachs, W. (2004) Ten Species in One: DNA Barcoding Reveals Cryptic

Species in the Neotropical Skipper Butterfly Astraptes fulgerator. *Proceedings of the National Academy of Sciences*, **101**, 14812–14817.

Hebert, P.D.N., de Waard, J.R. & Landry, J.-R. (2010) DNA barcodes for 1/1000 of the animal kingdom. *Biology Letters in Evolutionary Biology*, **6**, 359–362.

Huson, D.H. & Bryant, D. (2006) Application of phylogenetic networks in evolutionary studies. *Molecular Biology and Evolution*, **23**, 254–267.

Janzen, D. H., & Hallwachs, W. (2009) Dynamic database for an inventory of the macrocaterpillar fauna, and its food plants and parasitoids, of Area de Conservacion Guanacaste (ACG), northwestern Costa Rica (nn-SRNP-nnnnn voucher codes) Available at: http://janzen.sas.upenn.edu

Kass, R.E. & Raftery, A.E. (1995) Bayes factors. *Journal of the American Statistical Association*, **90**, 773–795.

Keightley, P.D., Pinharanda, A., Ness, R.W. *et al.* (2015) Estimation of the spontaneous mutation rate in Heliconius melpomene. *Molecular Biology and Evolution*, **32**, 239–243.

Klingenberg, C.P. (2010) Evolution and development of shape: integrating quantitative approaches. *Nature Reviews*, **11**, 623–635.

Klingenberg, C.P. (2011) MorphoJ: an integrated software package for geometric morphometrics. *Molecular Ecology Resources*, **11**, 353–357.

Kozak, K.M., Wahlberg, N., Neild, A.F.E., Dasmahapatra, K.K., Mallet, J. & Jiggins, C.D. (2015) Multilocus species trees show the recent adaptive radiation of the Mimetic *Heliconius* butterflies. *Systematic Biology*, **64**, 505–524.

Kronforst, M.R. (2005) Primers for the amplification of nuclear introns in *Heliconius* butterflies. *Molecular Ecology Notes*, **5**, 158–162.

Kumar, S., Stecher, G. & Tamura, K. (2016) MEGA7: Molecular Evolutionary Analysis Version 7.0 for bigger datasets. *Molecular Biology & Evolution*, **33**, 1870–1874.

Lamas, G. (2004) Checklist: Part 4A. Hesperioidea - Papilionoidea. *Atlas of Neotropical Lepidoptera. Volume 5A* (ed. by J.B. Heppner). Gainesville: Association for Tropical Lepidoptera; Scientific Publishers.

Lanfear, R., Calcott, B., Ho, S.Y.W. & Guindon, S. (2012) Partition finder: combined selection of partitioning schemes and substitution models for phylogenetic analyses. *Molecular Biology and Evolution*, **29**, 1695–1701.

Le Roy, C., Debat, V. & Llaurens, V. (2019) Adaptive evolution of butterfly wing shape: from morphology to behavior. *Biological Reviews*, **94**, 1261–1281.

Leaché, A.D. & Fujita, M.K. (2010) Bayesian species delimitation in West African forest geckos (*Hemidactylus fasciatus*). *Proceedings of the Royal Society B: Biological Sciences*, **277**, 3071–3077.

Leigh, J.W. & Bryant, D. (2015) POPART: full-feature software for haplotype network construction. *Methods in Ecology & Evolution*, **6**, 1110–1116.

Leisch, F., Hornik, K., & B.D. Ripley (2020) mda: Mixture and flexible discriminant analysis. R package version 0.5-2. Available at: https://CRAN.R-project.org/package=mda

Mallet, J. & Gilbert, L.E. (1995) Why are there so many mimicry rings? Correlations between habitat, behaviour and mimicry in *Heliconius* butterflies. *Biological Journal Linnean Society*, **55**, 159–180.

Martin, S.H., Dasmahapatra, K.K., Nadeau, N.J. *et al.* (2013) Genome-wide evidence for speciation with gene flow in *Heliconius* butterflies. *Genome Research*, **23**, 1817–1828.

Massardo, D., Fornel, R., Kronforst, M., Lopes-Goncalves, G. & Pires-Moreira, G.R. (2014) Diversification of the silverspot butterflies (Nymphalidae) in the Neotropics inferred from multi-locus DNA sequences. *Molecular Phylogenetics and Evolution*, **82**, 156–165.

Massardo, D., VanKuren, N.W., Nallu, S. *et al.* (2020) The roles of hybridization and habitat fragmentation in the evolution of Brazil's enigmatic longwing butterflies, *Heliconius nattereri* and *H. hermathena*. *BMC Biology*, **18**, 84.

Matos-Maraví, P., Wahlberg, N., Freitas, A.V.L., Devries, P., Antonelli, A. & Penz, C.M. (2021) Mesoamerica is a cradle and the Atlantic Forest is a museum of Neotropical butterfly diversity: insights from the evolution and biogeography of Brassolini (Lepidoptera: Nymphalidae). *Biological Journal of the Linnean Society*, **133**, 704–724. https://doi.org/10.1093/biolinnean/blab034.

Matos-Maraví, P.F., Wahlberg, N., Antonelli, A. & Penz, C.M. (2019) Species limits in butterflies (Lepidoptera: Nymphalidae): reconciling classical taxonomy with the multispecies coalescent. *Systematic Entomology*, **44**, 1–13.

Mérot, C., Debat, V., Le Poul, Y. *et al.* (2020) Hybridization and transgressive exploration of colour pattern and wing morphology in *Heliconius* butterflies. *Journal of Evolutionary Biology*, **33**, 942–956.

Michener, C.D. (1942) A review of the subspecies of *Agraulis vanillae* (Linnaeus) (Lepidoptera: Nymphalidae). *American Museum Novitates*, **1215**, 1–7.

Miller, L.D. & Steinhauser, S.R. (1992) Butterflies of the Cayman Islands, with the description of a new subspecies. *Journal of the Lepidopterists' Society*, **46**, 119–127.

Minno, M.C. & Emmel, T.C. (1993) *Butterflies of the Florida Keys*. Scientific Publishers, Gainesville.

Mora, A., Baby, P., Roddaz, M., Parra, M., Brusset, S., Hermoza, W. & Espurt, N. (2010) Tectonic history of the Andes and sub-Andean zones: implications for the development of the Amazon drainage basin. *Amazonia, Landscape and Species Evolution: A Look into the Past* (ed. by C. Hoorn and F.P. Wesselingh). Oxford: John Wiley and Sons.

Morris, J., Navarro, N., Rastas, P., Rawlins, L.D., Sammy, J., Mallet, J. & Dasmahapatra, K.K. (2019) The genetic architecture of adaptation: convergence and pleiotropy in *Heliconius* wing pattern evolution. *Heredity*, **123**, 138–152.

Mutanen, M., Hausmann, A., Hebert, P.D.N., Landry, J.-F., de Waard, J.R., & Huemer, P. (2012) Allopatry as a Gordian Knot for Taxonomists: Patterns of DNA Barcode Divergence in Arctic-Alpine Lepidoptera. *PLoS ONE*, **7**, e47214.

Nadeau, N.J., Martin, S.H., Kozak, K.M.,.R.H. *et al.* (2013) Genome-wide patterns of divergence and gene flow across a butterfly radiation. *Molecular Ecology*, **22**, 814–826.

Núñez, R., Genaro, J.A., Pérez-Asso, A. *et al.* (2020) Species delimitation and evolutionary relationships among *Phoebis* New World sulphur butterflies (Lepidoptera, Pieridae, Coliadinae). *Systematic Entomology*, **45**, 481–492.

O'Dea, A., Lessios, H.A., Coates, A.G. *et al.* (2016) Formation of the Isthmus of Panama. *Science Advances*, **2**, e1600883.

Ogilvie, H.A., Bouckaert, R.R. & Drummond, A.J. (2017) StarBEAST2 brings faster species tree inference and accurate estimates of substitution rates. *Molecular Biology and Evolution*, **34**, 2101–2114.

Ortiz-Acevedo, E., Gomez, J.P., Espeland, M., Toussaint, E.F.A. & Willmott, K.R. (2020) The roles of wing color pattern and geography in the evolution of Neotropical Preponini butterflies. *Ecology & Evolution*, **10**, 12801–12816.

Paim, A.C., Kaminski, L.A. & Moreira, G.R.P. (2004) Morfologia externa dos estágios imaturos de heliconíneos neotropicais: IV. *Dryas iulia alcionea* (Lepidoptera, Nymphalidae, Heliconiinae). *Iheringia. Série Zoologica*, **94**, 25–35.

Penz, C. & Krenn, H.W. (2000) Behavioral adaptations to pollen-feeding in *Heliconius* Butterflies (Nymphalidae, Heliconiinae): an experiment using *Lantana* flowers. *Journal of Insect Behavior*, **13**, 865–880.

Penz, C.M. & Williams, S.F. (2020) Wing morphology and body design in *Opsiphanes* and *Caligo* butterflies match the demands of male mating displays (Lepidoptera: Nymphalidae). *Annals of the Entomological Society of America*, **113**, 207–215.

Rasband, W. (2007) ImageJ 1.43u. Available at: http://rsb.info.nih.gov/ij

Revell, L.J. (2012) phytools: An R package for phylogenetic comparative biology (and other things). *Methods in Ecology and Evolution*, **3**, 217–223.

Rickard, M.A. (1968) Life history of *Dryas julia delia* (Heliconiidae). *Journal of the Lepidopterits Society*, **22**, 75–76.

Ricklefs, R. & Bermingham, E. (2007) Review: The West Indies as a laboratory of biogeography and evolution. *Philosophical Transactions of the Royal Society of London B Series*, **363**, 2393–2413.

Ricklefs, R.E. & Lovette, I.J. (1999) The roles of island area per se and habitat diversity in the species–area relationships of four Lesser Antillean faunal groups. *Journal of Animal Ecology*, **68**, 1142–1160.

Riley, N.D. (1926) Colaenis and Dione (Lep., Nymphalidae): A revisional note on the species. *Entomologist*, **59**, 240–245.

Rohlf, F.J. (2006) *TpsDig, version 2.10*. State University of New York, New York, Stony Brook. Available at: http://www.sbmorphometrics.org/soft-dataacq.html [accessed on 03 March 2021].

Rosser, N., Phillimore, A.B., Huertas, B., Willmott, K.R. & Mallet, J. (2012) Testing historical explanations for gradients in species richness in heliconiine butterflies of tropical America. *Biological Journal of the Linnean Society*, **105**, 479–497.

Runquist, E.B., Forister, M.L. & Shapiro, A.M. (2012) Phylogeography at large spatial scales: incongruent patterns of population structure and demography of Pan-American butterflies associated with weedy habitats. *Journal of Biogeography*, **39**, 382–396.

Salis, P., Lorin, T., Laudet, V. & Frédérich, B. (2019) Magic traits in magic fish: understanding color pattern evolution using reef fish. *TRENDS in Genetics*, **35**, 265–278.

Schlick-Steiner, B.C., Steiner, F.M., Seifert, B., Stauffer, C., Christian, E., & Crozier, R.H. (2010) Integrative Taxonomy: A Multisource Approach to Exploring Biodiversity. *Annual Review of Entomology*, **55**, 421–438.

Smith, B.T., McCormack, J.E., Cuervo, A.M. *et al.* (2014) The drivers of tropical speciation. *Nature*, **515**, 406–409.

Smith, D.S., Miller, L.D. & Miller, J.Y. (1994) *The Butterflies of the West Indies and South Florida*. Oxford University Press, New York, New York.

Solis-Lemus, C., Knowles, L.L. & Ane, C. (2015) Bayesian species delimitation combining multiple genes and traits in a unified framework. *Evolution*, **69**, 492–507.

Sperling, F.A.H. (2003) Butterfly molecular systematics: from species definitions to higher-level phylogenies. *Butterflies: Ecology and Evolution Taking Flight* (ed. by C.L. Boggs, W.B. Watt and P.R. Ehrlich). Chicago: University of Chicago Press.

Stichel, H.F.E.J. (1908) Lepidoptera Rhopalocera. Fam. Nymphalidae. Subfam. Dioninae. *Genera Insectorum*, **63**, 1–38.

Sukumaran, J. & Knowles, L.L. (2017) Multispecies coalescent delimits structure, not species. *Proceedings of the National Academy of Sciences*, **114**, 1607–1612.

Tatsuta, H., Takahashi, K.H., & Sakamaki, Y. (2018) Geometric morphometrics in entomology: Basics and applications. *Entomological Science*, **21**, 164–184.

Toussaint, E.F.A., Dias, F.M.S., Mielke, O.H.H. *et al.* (2019) Flight over the Proto-Caribbean seaway: Phylogeny and macroevolution of Neotropical Anaeini leafwing butterflies. *Molecular Phylogenetics & Evolution*, **137**, 86–103.

Turner, T. & Turland, V. (2017) *Discovering Jamaican Butterflies and Their Relationships Around the Caribbean*. Safety Harbor: Caribbean Wildlife Publications.

Van Belleghem, S.M., Papa, R., Ortiz-Zuazaga, H., Hendrickx, F., Jiggins, C.D., McMillan, W.O. & Counterman, B.A. (2017) patternize: An R package for quiantifying color pattern variation. *Methods in Ecology and Evolution*, **9**, 390–398.

Wahlberg, N., Leneveu, J., Kodandaramaiah, U., Peña, C., Nylin, Freitas, A.V.L. & Brower, A.V.Z. (2009) Nymphalid butterflies diversify following near demise at the Cretaceous/Tertiary boundary. *Proceedings of the Royal Society of London (B)*, **276**, 4295–4302.

Wang, T., Qi, D., Sun, S., Liu, Z., Du, Y., Guo, S., & Ma, J. (2019) DNA barcodes and their characteristic diagnostic sites analysis of Schizothoracinae fishes in Qinghai province. *Mitochondrial DNA Part A*. doi:10.1080/24701394.2019.1580273

Warren, A.D., Davis, K.J., Stangeland, E.M., Pelham, J.P., Willmott, K.R. & Grishin, N.V. (2017) Illustrated lists of American butterflies. Available at: http://www.butterfliesofamerica.com/ [Accessed 21st November 2020].

Yang, Z. (2015) The BPP program for species tree estimation and species delimitation. *Current Zoology*, **61**, 854–865.

Zelditch, M.L., Swiderski, D.L. & Sheets, H.D. (2012) *Geometric Morphometrics for Biologists*, 2nd edn, p. 478. Elsevier Academic Press, London.

Zhang, J., Cong, Q., Shen, J., Opler, P.A., & Grishin, N.V. (2019) Genomics of a complete butterfly continent. bioRxiv 829887. doi: https://doi.org/10.1101/829887.

Zhang, J., Cong, Q., Shen, J., Opler, P.A. & Grishin, N.V. (2020) Genomic evidence suggests further changes of butterfly names. *The Taxonomic Report*, **8**(7), 1–41.

Zou, S., Li, Q., Kong, L., Yu, H., & Zheng, X. (2011) Comparing the usefulness of distance, monophyly and character-based DNA barcoding methods in species identification: a case study of Neogastropoda. *PloS ONE*. https://doi.org/10.1371/journal.pone.0026619